Title: Subtypes of brain change in aging and their associations with cognition and Alzheimer's disease biomarkers

Authors: Elettra Capogna[a], Øystein Sørensen[a], Leiv Otto Watne[b,c], James Roe[a], Marie Strømstad[a], Ane Victoria Idland[d], Nathalie Bodd Halaas[d,n], Kaj Blennow[e-h], Henrik Zetterberg[e,f,i,j,k,l], Kristine Beate Walhovd[a,m], for the Alzheimer's Disease Neuroimaging Initiative*, for the Australian Imaging Biomarkers and Lifestyle flagship study of ageing**, Anders Martin Fjell[a,m], Didac Vidal-Piñeiro[a]

Author affiliations:

[a] Center for Lifespan Changes in Brain and Cognition, Department of Psychology, University of Oslo, 0373 Oslo, Norway

[b] Department of Geriatric Medicine, Akershus University Hospital, Lørenskog, Norway

[c] Institute of Clinical Medicine, Campus Ahus, University of Oslo, Oslo, Norway

[d] Oslo Delirium Research Group, Department of Geriatric Medicine, Oslo University Hospital, Oslo, Norway

[e] Institute of Neuroscience and Physiology, the Sahlgrenska Academy at University of Gothenburg, Mölndal, Sweden

[f] Clinical Neurochemistry Laboratory, Sahlgrenska University Hospital, Mölndal, Sweden

[g] Paris Brain Institute, ICM, Pitié-Salpêtrière Hospital, Sorbonne University, Paris, France

[h] Neurodegenerative Disorder Research Center, Division of Life Sciences and Medicine, and Department of Neurology, Institute on Aging and Brain Disorders, University of Science and Technology of China and First Affiliated Hospital of USTC, Hefei, P.R. China

[i] Department of Neurodegenerative Disease, UCL Institute of Neurology, London, UK

[j] UK Dementia Research Institute at UCL, London, UK

[k] Hong Center for Neurodegenerative Diseases, Hong Kong, China

[l] Wisconsin Alzheimer's Disease Research Center, University of Wisconsin School of Medicine and Public Health, University of Wisconsin-Madison, Madison, WI, USA

[m] Computational Radiology and Artificial Intelligence, Department of Radiology and Nuclear Medicine, Oslo University Hospital, Oslo, Norway

[n] Institute of Clinical Medicine, Campus Ullevål, University of Oslo, Oslo, Norway

*Data used in preparation of this article were obtained from the Alzheimer's Disease Neuroimaging Initiative (ADNI) database (adni.loni.usc.edu). As such, the investigators within the ADNI contributed to the design and implementation of ADNI and/or provided data but did not participate in analysis or writing of this report. A complete listing of ADNI investigators can be found at: http://adni.loni.usc.edu/wp-content/uploads/how_to_apply/ADNI_Acknowledgement_List.pdf

**Data used in the preparation of this article was obtained from the Australian Imaging Biomarkers and Lifestyle flagship study of ageing (AIBL) funded by the Commonwealth Scientific and Industrial Research Organisation (CSIRO) which was made available at the ADNI database (www.loni.usc.edu/ADNI). The AIBL researchers contributed data but did not

participate in analysis or writing of this report. AIBL researchers are listed at www.aibl.csiro.au.

Corresponding author:

Elettra Capogna

Department of Psychology, Pb. 1094 Blindern

Oslo, Norway, 0317

elettra.capogna@psykologi.uio.no

Phone number: (+47) 22845095

Running title: Brain ageotypes' associations with cognition and biomarkers

Abstract

Structural brain changes underly cognitive changes in older age and contribute to inter-individual variability in cognition. Here, we assessed how changes in cortical thickness, surface area, and subcortical volume, are related to cognitive change in cognitively unimpaired older adults using structural magnetic resonance imaging (MRI) data-driven clustering. Specifically, we tested (1) which brain structural changes over time predict cognitive change in older age (2) whether these are associated with core cerebrospinal fluid (CSF) Alzheimer's disease (AD) biomarkers phosphorylated tau (p-tau) and amyloid-β (Aβ42), and (3) the degree of overlap between clusters derived from different structural features. In total 1899 cognitively healthy older adults (50 - 93 years) were followed up to 16 years with neuropsychological and structural MRI assessments, a subsample of which (n = 612) had CSF p-tau and Aβ42 measurements. We applied Monte-Carlo Reference-based Consensus clustering to identify subgroups of older adults based on structural brain change patterns over time. Four clusters for each brain feature were identified, representing the degree of longitudinal brain decline. Each brain feature provided a unique contribution to brain aging as clusters were largely independent across modalities. Cognitive change and baseline cognition were best predicted by cortical area change, whereas higher levels of p-tau and Aβ42 were associated with changes in subcortical volume. These results provide insights into the link between changes in brain morphology and cognition, which may translate to a better understanding of different aging trajectories.

Keywords

Memory, Ageotypes, Longitudinal MRI, Cognitively unimpaired older adults, CSF AD biomarkers

1. Introduction

Cognitive changes in healthy aging are partly explained by age-related macrostructural brain changes that may be quantified using repeated structural magnetic resonance imaging (MRI) assessments (Fjell and Walhovd, 2010). However, the extent of age-related changes in brain and cognition differs among older individuals (Lindenberger, 2014), and such differences may be partly underpinned by different patterns of brain aging. The association between brain changes and cognitive change can be assessed by examining different features of morphometric changes, such as cortical thickness, surface area, and subcortical volume. These features have been associated with different aspects of cognition in aging (Nyberg et al., 2023), and with different cerebrospinal fluid (CSF) biomarkers of Alzheimer's disease (AD) pathology (Fjell et al., 2010; Pettigrew et al., 2016; Wang et al., 2015). MRI data-driven clustering approaches have proven useful for separating subgroups of healthy older participants ("ageotypes") with different biological, cognitive, and sociodemographic characteristics (Ahadi et al., 2020; Cox et al., 2021). Hence, in the present study, we applied a Monte-Carlo Reference-based consensus clustering algorithm (John et al., 2020) on longitudinal MRI brain features to identify subgroups of cognitively unimpaired older adults based on different structural brain change patterns over time. Moreover, we tested whether the different features of brain change were associated with cognitive changes and with core AD CSF biomarkers the 42 amino acid-long form of amyloid-β (Aβ42) and phosphorylated tau 181 (p-tau) to gain insight into whether brain changes in normal aging can potentially be explained by the presence of AD biomarkers.

In the aging context, longitudinal studies are necessary to capture inter-individual variability in structural brain changes (slope differences), because cross-sectional studies cannot separate aging-specific effects from earlier individual differences (intercept differences) in brain structural measures (Fjell et al., 2014a; Vidal-Piñeiro et al., 2022). This is also supported by a

study that found that the underlying factor structure for intercepts versus slopes across brain regions was different, and the correlation patterns between cortical volumetric change were stronger than those observed at baseline in cross-sectional analysis (Cox et al., 2021). Multiple timepoints and long follow-up times are critical to estimate the association between changes in the brain and cognition (Raz and Lindenberger, 2011), and to better understand the neurobiological mechanisms underlying specific cognitive aging processes (Cox et al., 2021; Fjell et al., 2014a).

The use of data-driven clustering, whether based on MRI or cognitive data, is beneficial in assessing the heterogeneity of changes in older participants. This approach was used by Josefsson et al. (2012) who identified ageotypes based on longitudinal trajectories of memory change over 15 years. Participants were divided into maintainers, decliners, and those showing average changes associated with age. Specific environmental and genetic characteristics (such as sex, variance in occupation, education, and physical activity) were related to each group.

Different morphometric features, such as cortical thickness, surface area, and subcortical volume, have been studied to describe inter and intra-individual variation in brain structures. The different features are thought to be largely unrelated to each other (Lemaitre et al., 2012) or even to be negatively associated, as in Storsve and colleagues (2014) where less decrements in cortical area were associated with more cortical thinning. Cortical thickness, cortical area, and subcortical volume decline in aging (Borgeest et al., 2021; Nyberg et al., 2023; Storsve et al., 2014); yet few studies have assessed longitudinal brain changes, taking into account the different brain features (Borgeest et al., 2021; Nyberg et al., 2023; Sele et al., 2021; Storsve et al., 2014). Indeed, cortical area and thickness seem to reflect distinct underlying neurobiological mechanisms that are differently affected in aging (Storsve et al., 2014), show

specific regional changes, and have a negative genetic correlation (Grasby et al., 2020). Assessing change in the different features of brain aging independently and considering to which degree they complement each other may translate to a better understanding of aging brain heterogeneity.

So far, there is inconclusive evidence regarding the association between structural brain changes and cognitive changes in aging, and most of the evidence is based on cross-sectional studies, with few exeptions. Thickness, but not area, changes were related to fluid intelligence changes (Sele et al., 2021) and memory changes, especially in the medial temporal lobe, as described in one study (Fjell et al., 2014b). Other studies found that surface area changes were associated with changes in proxy measures of fluid intelligence (Borgeest et al., 2021). Nyberg et al. (2023) described a significant association of surface area changes with a speed of processing test. Another study found positive associations between a general cognitive ability (GCA) factor and brain features, but with different results: indeed, higher baseline GCA was associated with greater cortical area at baseline and less cortical thinning over time (Walhovd et al., 2022). Finally, there is a general agreement in the literature regarding the positive association between hippocampal volume loss and episodic memory decline (Capogna et al., 2023a; Gorbach et al., 2020, 2017; Persson et al., 2012).

Decreased CSF Aβ42 (reflecting amyloid accumulation in the brain tissue) and increased p-tau (reflecting a neuronal response to Aβ pathology) concentrations are considered two of the key biomarker hallmarks of AD pathology (Jack et al., 2018), and their changes are identified in the early stage of the AD continuum, without the presence of any cognitive symptoms. Hence, it is relevant to understand the relationship between these biomarkers and the different structural features of brain change in cognitively unimpaired older adults, to better identify how these brain changes may be explained by the presence of AD biomarkers along an aging-

157 disease continuum. CSF Aβ42 and p-tau biomarker changes have been associated with lower
158 cortical thickness and subcortical volume atrophy in AD-vulnerable regions in cognitively
159 unimpaired older adults (Arenaza-Urquijo et al., 2013; Pettigrew et al., 2016; Wang et al.,
160 2015). However, the relationship between CSF Aβ42 and brain atrophy is inconclusive (Fjell
161 et al., 2014a), whereas p-tau shows a stronger association with medial temporal lobe (MTL)
162 atrophy, following the time course of cognitive decline (Pettigrew et al., 2017; Vidal-Piñeiro
163 et al., 2022; Wisse et al., 2022). To our knowledge, no study has explored the relationship
164 between CSF core AD biomarkers and surface area changes. Moreover, early CSF Aβ42 and
165 p-tau biomarker changes (notably for p-tau, unclear for Aβ42 (Parent et al., 2023)) have been
166 described as predictive of future cognitive decline, especially in episodic memory, although
167 the overall effects were small (Clark et al., 2018; Hedden et al., 2013; Stomrud et al., 2007).

168 In the present study, we investigated the inter-individual patterns of structural brain changes in
169 normal aging using a consensus clustering algorithm. This approach allowed us to identify
170 subgroups, i.e. clusters, among older participants. We used different indices of brain
171 morphology, namely cortical thickness, cortical area, and subcortical volume to better
172 understand the degree to which each modality contributes independently to brain longitudinal
173 decline, and the degree of overlap across them. Moreover, we assessed whether the clusters
174 were related to different trajectories of episodic memory function and global cognition, as
175 measured by dementia screening tools. Finally, we tested the associations between brain
176 changes and baseline concentrations of core AD CSF biomarkers (Aβ42 and p-tau, as well as
177 the p-tau/Aβ42 ratio).

178

179

180 ## 2 Material and methods

181

2.1 Participants

The total sample included 1899 cognitively healthy older participants (1080 females, mean age = 69.88 years, standard deviation [SD] = 7.90, age range = 50.11 – 93.01 years) from 7 cohorts: COGNORM (Idland et al., 2017), the Alzheimer's Disease Neuroimaging Initiative (ADNI) (Mueller et al., 2005), the Open Access Series of Imaging Studies (OASIS3) (LaMontagne et al., 2019), the Australian Imaging, Biomarker & Lifestyle Flagship Study of Ageing (AIBL) (Ellis et al., 2009), the Harvard Aging Brain Study (HABS) (Dagley et al., 2017), the Pre-symptomatic Evaluation of Novel or Experimental Treatments for AD (PREVENT-AD) program (Breitner et al., 2016; Tremblay-Mercier et al., 2021), and the Center for Lifespan Changes in Brain and Cognition (LCBC) dataset (Fjell et al., 2023). Data were collected by previously cited groups. See **Table 1** for more details on each dataset. The common inclusion criteria were as follows: minimum age of 50 years, total follow-up time of at least 1 year, and inclusion of scanners with 15 or more measurements to reduce noise and bias in the analysis. Moreover, the participants were required to be cognitively unimpaired at baseline according to a battery of neuropsychological tests. See specific inclusion criteria for each cohort in Supplementary Information (**SI**). Longitudinal structural MRI scans were available for up to 15.84 years (mean = 4.81 [2.81] years). At baseline, participants showing concurrent mild cognitive impairment, AD, or other severe neurological disorders were excluded from the analysis. All participants provided written informed consent, and the studies were approved by the relevant ethical committees and conducted in accordance with the Declaration of Helsinki.

203 **Table 1 Cohort characteristics**

	COGNORM	ADNI	OASIS 3	AIBL	HABS	PREVENT-AD	LCBC	Total
N (F:M)	95 (52:43)	544 (293:251)	518 (292:226)	149 (75:74)	166 (99:67)	229 (161:68)	198 (108:90)	1899 (1080:819)
Mean Age	73.40 (6.21)	73.22 (5.98)	69.00 (8.41)	71.09 (6.34)	72.78 (6.04)	63.56 (5.03)	65.23 (9.64)	69.88 (7.90)
Age range	64.74 – 89.79	55.80 – 89.90	50.11 – 93.01	60.00 – 87.00	62.50 – 87.75	55.13 – 84.22	50.39 – 84.47	50.11 – 93.01
Time MRI follow-up	5.94 (2.61)	4.12 (2.68)	5.13 (3.35)	4.04 (1.62)	4.88 (0.97)	2.88 (1.13)	6.30 (2.80)	4.81 (2.81)
MRI obs (n)	370 (3.90 [1.36])	2492 (4.58 [2.42])	1652 (3.19 [1.49])	498 (3.34 [1.10])	504 (3.04 [0.53])	1203 (5.23 [1.39])	574 (2.90 [0.83])	7293 (3.84 [1.86])
Global cognition obs (n)	609 (6.41 [0.99])	2614 (4.80 [2.52])	3584 (6.96 [3.98])	598 (4.01 [1.17])	988 (5.95 [0.21])	229 (1 [0])	525 (2.65 [0.86])	9147 (4.54 [1.39])
Memory obs (n)	609 (6.41 [0.99])	2836 (5.21 [2.67])	493 (4.48 [2.68])	507 (3.40 [1.13])	993 (5.98 [0.80])	969 (4.25 [1.39])	420 (2.80 [0.79])	6827 (4.64 [1.49])
Education (years)	14.94 (3.97)	16.50 (2.56)	15.89 (2.63)	-	16.14 (3.01)	15.25 (3.27)	16.04 (2.77)	15.97 (2.88)

***APOE* ε4** (-/+)	48:37	368:170	332:186	99:50	118:46	146:83	50:21	1161:593

Descriptive statistics represent mean (SD). N = number of subjects. Obs = total number of observations. *The MRI obs* row shows the mean ([SD]) of the number of observations per participant and the total number. The same applies to global cognition and memory. Note that the term "global cognition" specifically pertains to the screening tests outlined below. *APOE* ε4 = non-carriers:carriers. Participants with heterozygous or homozygous ε4 alleles were regarded as carriers.

208

209 ## 2.2 MRI acquisition and preprocessing

210 Structural T1-weighted (T1w) MPRAGE scans were collected using 1.5 and 3 T scanners. See
211 information on scanner parameters and scanners per dataset in the SI. Images were transformed
212 into the Brain Imaging Data Structure (BIDS) format (Gorgolewski et al., 2016). Clinica
213 software was used for the ADNI, AIBL, and HABS BIDS transformations (Routier et al., 2021;
214 Samper-González et al., 2018). We used the longitudinal FreeSurfer v.7.1.0 stream (Reuter et
215 al., 2012) for cortical reconstruction of the structural T1w scans (Dale et al., 1999; Fischl et al.,
216 1999). Briefly, the images were processed using the cross-sectional stream, which includes the
217 removal of nonbrain tissues, Talairach transformation, intensity correction, tissue and
218 volumetric segmentation, cortical surface reconstruction, and cortical parcellation. Next, an
219 unbiased within-subject template space based on all cross-sectional images was created for
220 each participant, using robust, inverse-consistent registration (Reuter et al., 2010). The
221 processing of each time point was then reinitialized with common information from the within-
222 subject template, to increase reliability and statistical power. Data were summarized based on
223 the Destrieux atlas (Destrieux et al., 2010) for cortical thickness and cortical area measures (74
224 features) and the *aseg* atlas for subcortical volumetric data (17 features) (Fischl et al., 2002).

225

226 ## 2.3 Computation of intercept and slope measures for ROIs per participant

227 We focused on three indices of cerebral morphology: cortical thickness, surface area, and
228 subcortical volume. For each region of interest (ROI), we regressed out the effects of mean age
229 across timepoints for each participant using generalized additive mixed models (GAMM)
230 (Wood, 2017), as implemented in the *gamm4* package. Age was introduced as a smooth term,
231 while random intercepts were included for each dataset, scanner, and participant. To compute
232 the slope of change for each participant, we fit a linear regression model for each participant

and ROI with the GAMM model residuals (as dependent variable) and time equal to the difference between age at a given observation and the individual's mean age. Participants without longitudinal MRI data and those with follow-up intervals of < 1 year were excluded from further analysis and were not included in the final sample. Next, we replaced outlier values (> ±5 SD from the mean) using the *mice* package (Buuren and Groothuis-Oudshoorn, 2011) (0.003% of observation values were replaced). The final output yielded a total of 330 structural MRI features (148 cortical thickness, 148 surface area, and 34 subcortical volumetric bilateral ROIs that contained slope data). Finally, the values were scaled for each feature.

2.4 Consensus clustering of brain data

Slope data were clustered based on the M3C clustering algorithm – a Monte-Carlo Reference-based Consensus algorithm - as implemented in the *M3C* package (John et al., 2020). Consensus algorithms (Monti et al., 2003) are based on the idea that the ideal cluster should be stable despite resampling, that is, that individuals should always or never be clustered together in the face of iterative resampling. Such methods have gained popularity as they produce more robust results, reduce bias, and provide estimates of the error.

An important challenge in consensus clustering is selecting the number of clusters (K). The most popular criteria either require subjective decisions or show biases towards small or high K-solutions. Furthermore, most approaches cannot test whether the desired solution is better than K = 1 (i.e., that the data comes from a single distribution). M3C solves both problems by generating Monte Carlo simulations that preserve the covariance structure. M3C provides null stability scores for a range of K values, which are then compared with real-data solutions. Here, we used the Relative Cluster Stability Index (RCSI) metric to select K based on the proportion of ambiguous clusters (PAC) scores. RCSI p-values were further derived to test the null

hypothesis of K = 1 at each value of K. We used a spectral clustering algorithm (Ng et al., 2001) as it is capable of coping with complex data structures. The remaining parameters were set to the default values of *M3C* version 1.24.0. The algorithm was separately applied to each of the three morphometric brain measures. To explore the data structure, we projected the cluster outcome (i.e., individual assignments) onto main components of brain change (i.e., components capturing the main axis of variability of brain data) (n = 4) and carried out an ANOVA using cluster assignment as the factor of interest. When significant (Bonferroni-corrected), post-hoc pairwise comparisons were performed. Finally, for each cluster and feature, we estimated the mean values.

2.5 Degree of overlap between cluster solutions

We carried out an analysis to establish whether the different structural modalities were statistically related to each other, i.e., whether participants belonged to different clusters or the same cluster across the various morphometric brain features. The explorative analysis indicated that clustering was based on one principal component from a Principal Component Analysis (PCA), and all the clustering solutions resulted in four groups. See **Supplementary Figure 1**. Thus, for clarity, we renamed the clusters based on their mean ROIs change values as follows: Decline, Mild Decline, Mild Maintenance, Maintenance. Cohen's kappa was used to assess the agreement among clusters, as implemented in the *psych* and *irr* R-packages. A weighted kappa coefficient was applied because of the ordinal characteristics of the clusters and to stress the large discrepancies in ratings more than the small ones (Sim and Wright, 2005).

2.6 Cognitive functions over time

We focused on memory and global cognitive impairment because of their relevance in aging. For the global cognitive impairment factor, we used the longitudinal scores from the Mini-Mental State Examination (MMSE) (Folstein et al., 1975) for all samples except PREVENT-AD, for which the Montreal Cognitive Assessment (MOCA) was used (Nasreddine et al., 2005). We used these screening tests as a global measure of cognitive function (Garcia-Diaz et al., 2014; Matsushima et al., 2015), acknowledging their sensitivity to dementia and cognitive decline in the aging-disease continuum. The number of participants included was n = 1896. Within cohorts, we scaled the longitudinal scores based on the mean and SD at the first time point (same procedure applied below for the memory scores). Note that PREVENT-AD did not include longitudinal MOCA scores. Moving forward, we will collectively refer to the output of these screening tests as 'global cognition', as they are both sensitive to premorbid global cognitive decline. For the memory factor, we selected the precomputed ADNI-MEM (Crane et al., 2012) for the ADNI dataset. For the other datasets, we used the Immediate and Delay scores in the Word List Memory Task (CERAD) (Morris et al., 1989) for COGNORM, and the short delay and delayed score of the Logical Memory Test (Wechsler, 1987) for AIBL, HABS, and OASIS3. For PREVENT-AD, we used the memory index score (Immediate and Delayed) obtained from the Repeatable Battery for Assessment of Neuropsychological Status (RBANS) (Randolph et al., 1998; Tremblay-Mercier et al., 2021) and the short delay, delayed, and total learning from the California Verbal Learning Test (Delis et al., 2000) for LCBC. Then we performed separate PCA on the first timepoint in each dataset with multiple memory variables. The loadings for the first component were used to calculate scores for the first principal component across all timepoints (Capogna et al., 2023b). The *prcomp* function was used for the PCA. Furthermore, for both memory and global cognition factors, we regressed the effects of age using GAMMs (Wood, 2017). Age was introduced as a smooth term and a

test-retest variable as a dichotomic covariate to account for training effects (Capogna et al., 2023b), and random intercepts were included for each participant in the model. To compute the slope, we first extracted the residuals from the GAMMs, and then we ran a linear regression model for each participant with age as the predictor and residuals as outcome. For the global cognition factor, longitudinal results were available for 1649 participants, and the memory change factor for 1442 participants.

2.7 CSF collection, analysis and computation of intercept and slope

CSF data were available for three cohorts: ADNI, COGNORM, and PREVENT AD (total number of participants available = 612). For ADNI, CSF Aβ42 and p-tau concentrations were measured using Elecsys phosphorylated-tau 181 (p-tau) and β-amyloid (Aβ42) CSF immunoassays (*UPENNBIOMK9.csv* ADNI file). CSF collection for COGNORM has been thoroughly described previously (Idland et al., 2017). Briefly, CSF samples were analyzed at the Clinical Neurochemistry Laboratory of Sahlgrenska University Hospital (Mölndal, Sweden). CSF concentrations of Aβ42 and p-tau were measured using the INNOTEST enzyme-linked immunosorbent assay (ELISA; Fujirebio, Ghent, Belgium). CSF collection for PREVENT-AD has been described previously (Tremblay-Mercier et al., 2021). CSF samples for Aβ42 and p-tau 181 were measured using an INNOTEST enzyme-linked immunosorbent assay. We had 608 and 611 cross-sectional values for p-tau and Aβ42 respectively, and longitudinal values available for 327 and 328 participants for p-tau and Aβ42, respectively. Within each cohort, we first scaled each CSF value based on the mean and SD at the first timepoint. To compute the intercept and slope measure for CSF biomarkers, we fitted a linear regression model for each participant with the CSF scaled value as the dependent variable and time equal to the difference between age at a given observation and age at baseline. Due to the relatively small number of participants with longitudinal CSF data, the longitudinal biomarkers

329 analyses are deemed exploratory (see **Supplementary Table 3**). See **Table 2** for descriptive
330 CSF data.

331

332 **Table 2 Cross-sectional and longitudinal info CSF AD biomarkers**

	ADNI	**PREVENT-AD**	**COGNORM**
N	412	106	94
CSF p-tau bsl (pg/mL)	21.51 (8.74)	48.16 (17.67)	61.40 (18.96)
CSF Aβ42 bsl (pg/mL)	1359.10 (649.67)	1152.40 (270.77)	729.48 (205.77)
Time from first MRI (years)	1.47 (2.24)	1.43 (1.33)	0 (0)
Interval follow- up (range in years)	-3.74– 10.28	0.22 – 4.58	2.88 – 5.69
N follow-up	221	76	34
CSF p-tau total obs	802	351	66
CSF Aβ42 total obs	809	350	66

333 N = number of participants (with MRI available for clustering) with AD biomarkers available.
334 Bsl = baseline value. The Time variable represents the mean (SD) of years between CSF
335 collections and baseline first MRI measurement. The interval follow-up refers to the range of
336 Time (see above) in years of CSF longitudinal collections, excluding the first CSF assessment.
337 N follow-up represents the number of participants with at least 2 CSF measurements over time.
338 Obs = number of total observations for each CSF biomarker of interest.

339

340 ## 2.8 Statistical Analysis

341 All analyses were performed in the R environment (R Core Team, 2022). A chi-square test was
342 used to assess whether the clusters were associated with specific socio-demographic variables

such as Sex, *APOE* ε4, and Cohort variables. We used the *chisq.posthoc.test* package (Beasley and Schumacker, 1995) to assess the cluster driving the significant associations. Linear mixed-effects models (LME), as implemented in the *lme4* R-package (Bates et al., 2015), were used to assess whether the cluster assignments differed in education and mean age levels. Moreover, we used LME to compute the effect of cluster assignment on memory and global cognition intercept and change. Sex and mean age were introduced as covariates of no interest. Random intercepts per cohort were also included. In addition, 4-group ANOVA models were run on the outputs of the LME models. The models were corrected for multiple comparisons using the false discovery rate and Benjamini-Hochberg correction (pFDR) (Benjamini and Hochberg, 1995). Specifically, we corrected the p-values from all the models separately for each dependent domain (memory, global cognition, and CSF AD biomarkers). If the output was significant, we applied multiple comparisons of means, as implemented in the *multcomp* R-package (Westfall, 2010), that displayed the adjusted p-values, using a single-step method. The same procedure described above was run in a subsample (n = 612) to assess the relationship of brain change clusters with the CSF AD biomarkers. In the p-tau model, we also included baseline CSF Aβ42 as a covariate. We also tested the association with the p-tau/Aβ42 ratio.

2.9 Automated model selection

We tested the combined effects of cluster assignments (for changes in thickness, area, and subcortical volume) and their interactions on explaining memory, global cognition, CSF AD biomarkers, intercept, and slope (except for core CSF AD biomarkers). We used a LASSO algorithm (Tibshirani, 1996), that performs a variable selection to maximize the prediction accuracy, as implemented in the *gglasso* package (Yang and Zou, 2015) to automatically identify the best-performing model to explain the cognitive and biomarker changes. We used grouped LASSO to model the categorical properties of clusters, that is, both the different

368 regressors for the main effects of clusters and their interactions were grouped, so the outcome
369 either provided coefficients for all the conditions or none. First, we created a matrix of
370 predictors (X) containing the main effects and all the interactions among clusters, while we set
371 Sex and mean Age as fixed variables. We defined the response (y) as the cognitive or AD
372 biomarkers of interest in prediction. We applied the function *cv.gglasso*, employing 10-folds
373 cross-validation to determine the optimal smoothing λ parameter. We report the results at two
374 different λ: λ at minimum RMSE, and at the largest value of λ within 1 standard error of λ
375 minimum which leads to more conservative results.

376

377

378 3. Results

379

380 3.1 Clustering solutions for brain features and mean values of each cluster

381 We identified 4 clusters for each brain feature of interest. See **Figure 1** for a visual
382 representation of the results and SI in [Zenodo] at https://doi.org/10.5281/zenodo.10365469
383 for the stats of the three features. The PCA and the visual exploration of the results suggested
384 that clusters were defined based on a main axis (component) of decline. See **Supplementary**
385 **Figure 1.** We reordered the clusters from those showing a steeper overall decline to those that
386 displayed – comparatively – less decline. For cortical thickness change, we found a high effect
387 of bilateral temporal and inferior parietal regions on cluster assignment. To some degree, we
388 observed a similar pattern for surface area changes, although weaker and more prominent in
389 the left superior frontal and temporal regions. Subcortical volume cluster assignment was
390 especially influenced by hippocampus decline and ventricular expansion. Henceforth, the
391 clusters are renamed as decline, mild decline, mild maintenance, and maintenance. See **Figures**

392 **2, 3**, and **4** for a visual representation of the differences between the different clusters in each
393 analysis.

394

395 **Figure 1 ANOVA output of cluster assignment**

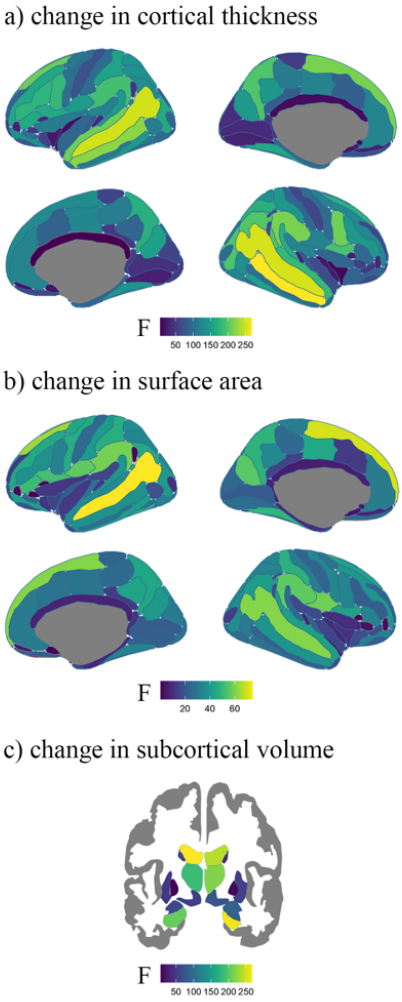

396

397 ANOVA output of brain change respectively for cluster assignments of cortical thickness,
398 surface area, and subcortical volume. The F-values represent the influence of each region in
399 the cluster assignment. Yellow regions represent more importance and blue regions represent
400 less importance. ROIs were based on the Destrieux atlas (Destrieux et al., 2010) for cortical

401 thickness and cortical area, and the *aseg* atlas (Fischl et al., 2002) for subcortical volumetric
402 data.

403

404 **Figure 2 Mean values for cortical thickness change in each cluster**

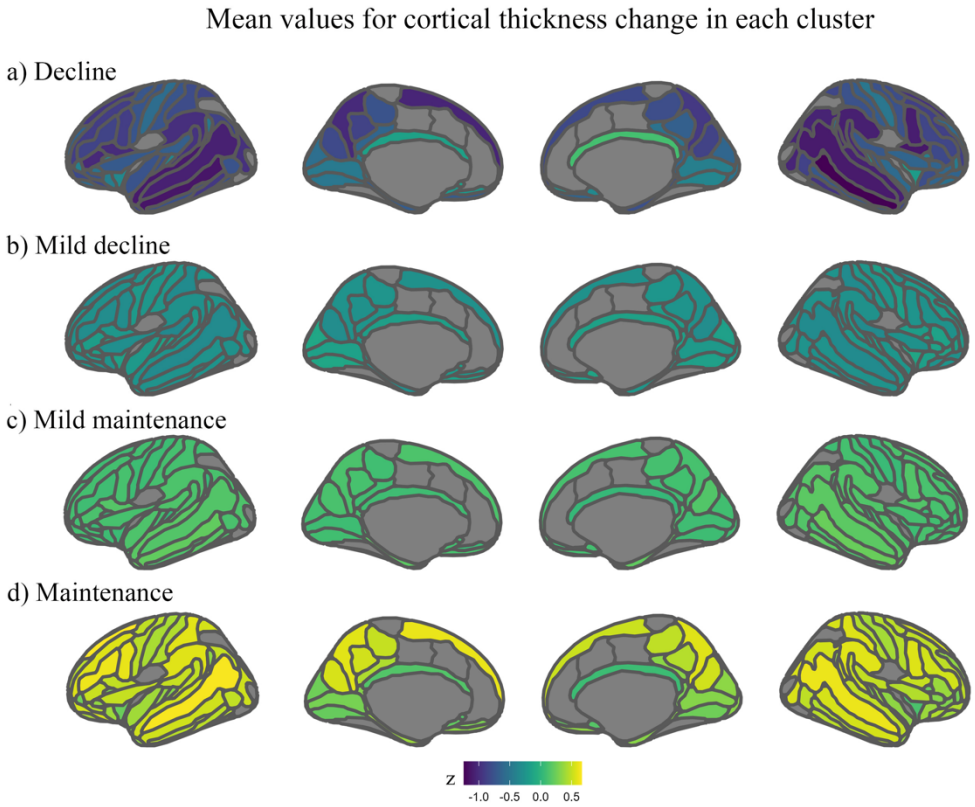

405

406 Mean thickness change (z scores) values for each of the four clusters. Yellow represents more
407 positive values and less change in thickness over time, while indigo represents more negative
408 values and more thinning over time. A) decline cluster; b) mild decline cluster; c) mild
409 maintenance cluster; d) maintenance cluster. ROIs were based on the Destrieux atlas (Destrieux
410 et al., 2010) for cortical thickness. ROIs without an overlay are not significant (pFDR < 0.05).

411

412 **Figure 3 Mean values for surface area change in each cluster**

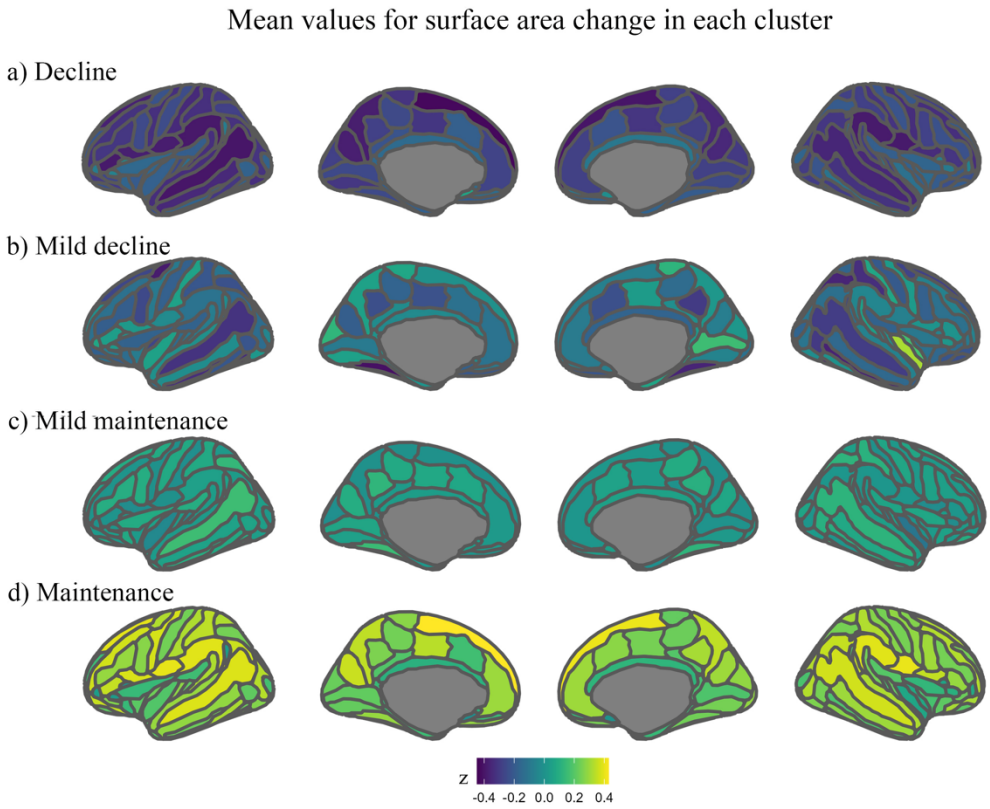

Mean area change (z scores) values for each of the four clusters. Yellow represents more positive values and less change in area over time, while indigo represents more negative values and more change in area over time. A) decline cluster; b) mild decline cluster; c) mild maintenance cluster; d) maintenance cluster. ROIs were based on the Destrieux atlas (Destrieux et al., 2010) for surface area. ROIs without an overlay are not significant (pFDR < 0.05).

Figure 4 Mean values for subcortical volume change in each cluster

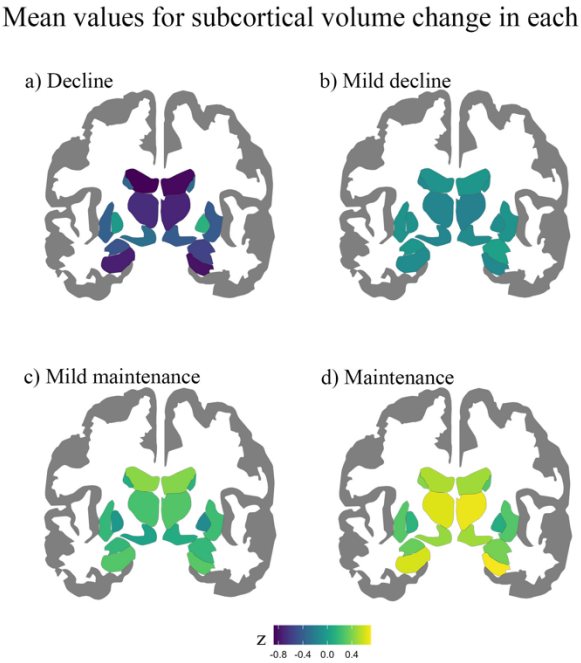

Mean subcortical change (z scores) values for each of the four clusters. Yellow represents more positive values and less change in subcortical volume, while indigo represents more negative values and more subcortical volume decline. A) decline cluster; b) mild decline cluster; c) mild maintenance cluster; d) maintenance cluster. ROIs were based on the *aseg* atlas (Fischl et al., 2002). ROIs without an overlay are not significant (pFDR < 0.05).

3.2 Degree of overlap between brain features

We next tested whether participants belonged to different clusters or the same cluster across the various morphometric brain measures. The cluster assignment for each brain feature is summarized in **Figure 5**. The weighted Cohen's kappa coefficient for correspondence in cluster assignment for thickness and area is $\kappa = 0.08$ ($p < 0.001$), which means that the agreement between clustering of different modalities was slight (as per Landis and Koch, 1977). This suggests, as also previously reported, that thickness and surface area are two largely unrelated and independent morphometric characteristics of aging (Storsve et al., 2014). The agreement between participants being classified on the same clusters for subcortical volume and thickness

437 is weighted $\kappa = 0.29$ ($p < 001$), often interpreted as "fair" (Landis and Koch, 1977), whereas

438 the weighted Cohen's kappa coefficient for subcortical volume and area is $\kappa = 0.19$ ($p < 0.001$).

439

440

441

442

443

444

445

446

447

448

449

450

451

452

453

454

455 **Figure 5 Contingency tables for brain cluster assignment**

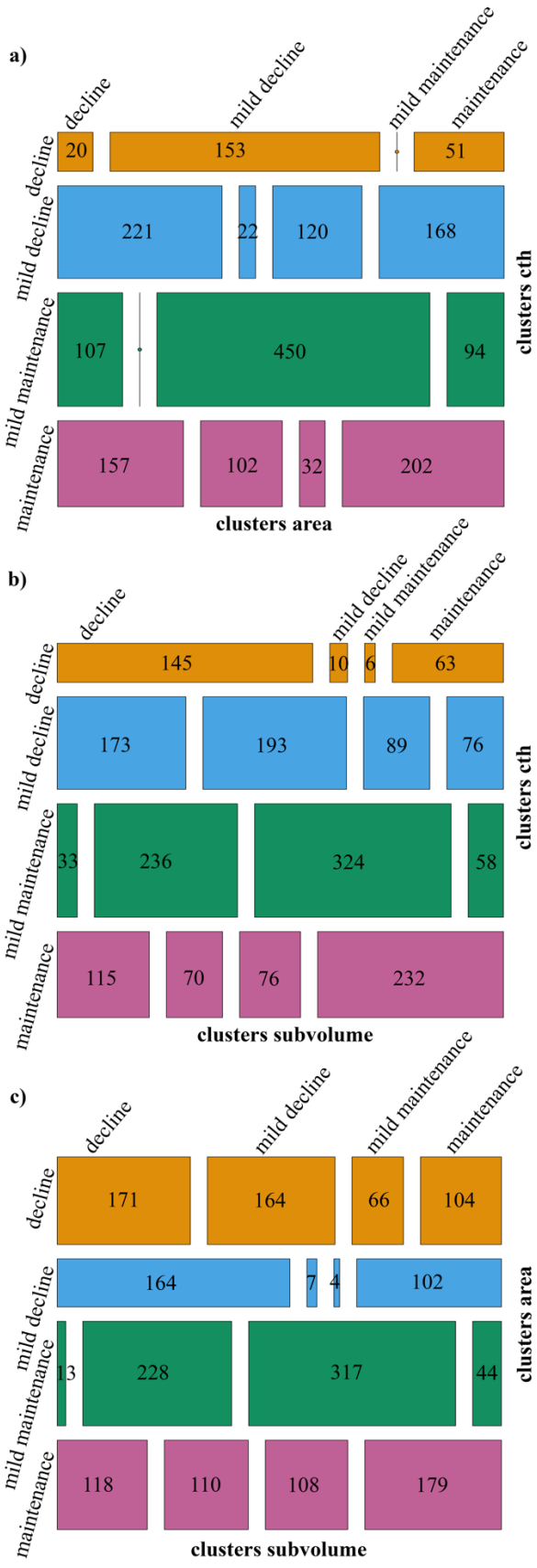

456

Mosaic plots reflecting the output of the contingency tables (*vcd R* package). The dimensions of each box are proportional to the number of participants grouped into the clusters based on the different structural modality. The kappa value is calculated based on the discrepancy between the diagonal boxes and those that are not located on the diagonal (agreement vs. disagreement). Cells without a number mean 0 participants belonged to the two different clusters. A) Table for clusters based on thickness change versus clusters based on area change; b) table for clusters based on thickness change versus clusters based on subcortical volume change; c) table for clusters based on area change versus clusters based on subcortical volume change.

3.3 Associations between brain cluster assignment and genetic-environmental variables

We then assessed whether the cluster assignment (for brain feature) differed for sex, age, education, *APOE* ε4 status, and cohort. No associations were found with education level. Changes in cortical thickness (cluster assignment) were associated with age ($F = 10.97$, $df1 = 1888.8$, $df2 = 3$, $pFDR < 0.001$), and *APOE* ε4 status ($\chi^2 = 11.86$, df residual = 1751, $pFDR = 0.01$). Changes in cortical surface clusters were related to age ($F = 32.56$, $df1 = 1889$, $df2 = 3$, $pFDR < 0.001$), sex ($\chi^2 = 41.44$, df residual = 1896, $pFDR < 0.001$), and *APOE* ε4 status ($\chi^2 = 15.34$, df residual = 1751, $pFDR < 0.01$). Changes in subcortical volume clusters were also related to age ($F = 19.98$, $df1 = 1889.5$, $df2 = 3$, $pFDR < 0.001$), sex ($\chi^2 = 52.15$, df residuals = 1896, $pFDR < 0.001$), and *APOE* ε4 status ($\chi^2 = 19.53$, df residual = 1751, $pFDR < 0.001$). Overall, the ANOVA results were in the expected direction, with clusters showing relative brain maintenance having lower age, lower representation of *APOE* ε4 carriers, and less males, whereas clusters showing more brain decline had higher age and a higher representation of *APOE* ε4 carriers and males. See **Supplementary Table 1** for the direction of the significant

post-hoc associations between cluster assignment and these genetic and environmental variables.

3.4 Associations between brain cluster assignment and cognitive functions

We then assessed the relationship between cluster assignment, intercept and change in memory and global cognition, using LME and 4-group ANOVA models. The results are presented in **Table 3** (including the post-hoc multiple comparisons), for a visual representation see **Figure 6.** We found significant associations between global cognition intercept and changes in cortical area ($F = 15.69$, $df1 = 1889$, $df2 = 3$, $pFDR < 0.001$), thickness ($F = 16.21$, $df1 = 1889$, $df2 = 3$, $pFDR < 0.001$), and subcortical volume ($F = 15.88$, $df1 = 1889$, $df2 = 3$, $pFDR < 0.001$). The ANOVA results were in the expected direction, with clusters showing relative brain maintenance displaying higher cognition, and those showing more brain decline exhibiting lower cognition. See the post-hoc comparisons across groups, that is, which specific clusters had significantly different values in **Table 3** and **Supplementary Table 2**. Global cognition changes were associated with surface area changes (cluster assignment) over time ($F = 4.16$, $df1 = 1605.9$, $df2 = 3$, $pFDR = 0.009$, post-hoc: lower cognition for mild decline cluster). No significant relationship between cluster assignment and memory change and intercept survived correction for multiple comparisons; all the results were above $pFDR > 0.05$.

Table 3 Associations between brain cluster assignment and cognitive functions

	Cognitive function	(F [pFDR])	η^2 partial
Cluster change thickness	Memory change	3.40 (0.10)	7.05×10^{-3}

	Memory intercept	0.77 (0.67)	1.61×10^{-3}
	Global cognition change	1.73 (0.16)	3.35×10^{-3}
	Global cognition intercept	16.21 (< 0.001) [-a,c]	0.02
Cluster change area	Memory change	0.85 (0.67)	1.78×10^{-3}
	Memory intercept	2.64 (0.14)	5.50×10^{-3}
	Global cognition change	4.16 (0.009) [-b]	7.71×10^{-3}
	Global cognition intercept	15.69 (< 0.001) [-b,c]	0.02
Cluster change subvolume	Memory change	0.51 (0.67)	1.08×10^{-3}
	Memory intercept	0.52 (0.67)	1.09×10^{-3}
	Global cognition change	1.84 (0.16)	3.62×10^{-3}
	Global cognition intercept	15.88 (< 0.001) [-a,b,c]	0.02

ANOVA models on the LME models output. Sex and Age at baseline (mean-centered) as covariates of no interest. Statistics represent F-values, pFDR corrected values, and η^2 partial represents the effect size eta squared partial. The superscripts represent the significant output ($p < 0.01$) of the post hoc multiple comparisons, where each cluster assignment is compared against all: a) decline cluster > mean; b) mild decline > mean; c) mild maintenance > mean; d) maintenance > mean. A negative sign indicates that the significant comparison was lower than the mean. Please note that the term "global cognition" specifically pertains to the aforementioned screening tests.

Figure 6 Significant associations between brain cluster assignment and global cognition

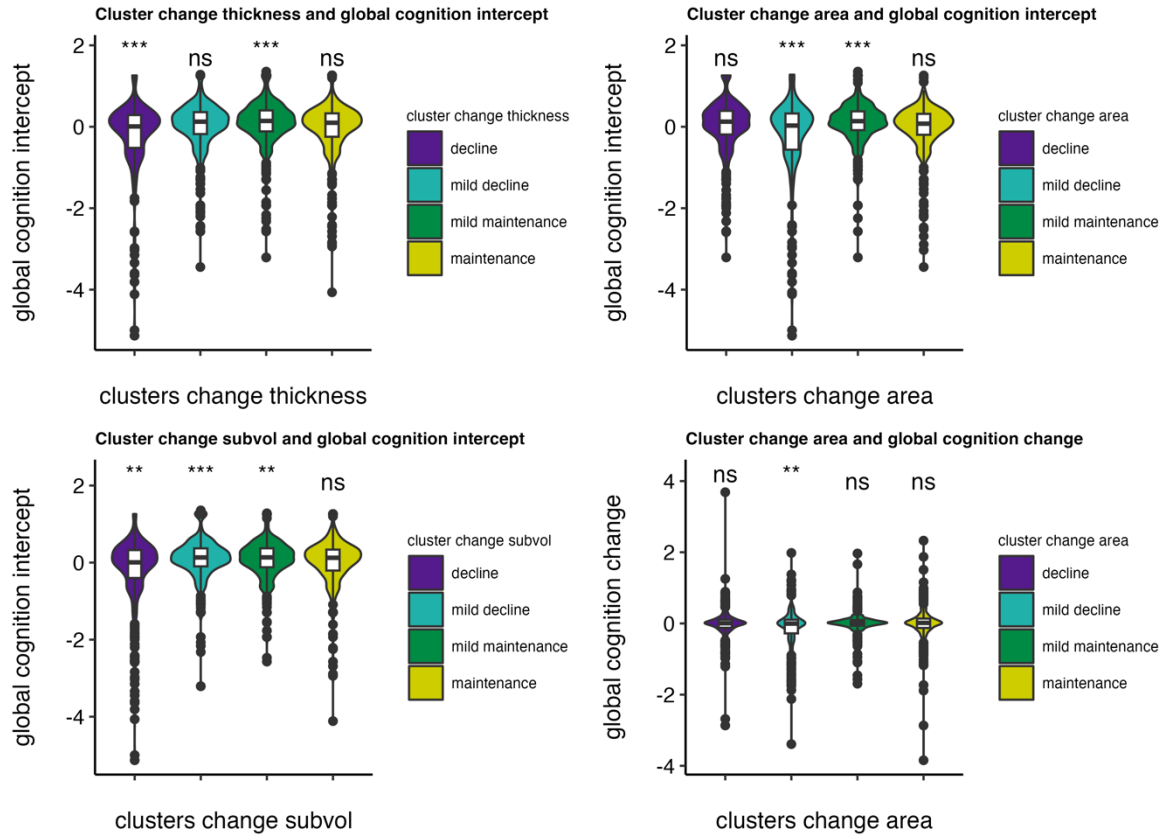

Post-hoc comparisons of means (one cluster vs. all) for global cognition intercept and change. ** = $p < 0.01$, *** = $p < 0.001$, ns = non-significant. Note that the term "global cognition" specifically pertains to the aforementioned screening tests.

3.5 Associations between brain cluster assignment and CSF AD biomarkers

The results are presented in **Table 4** (n = 612). Changes in subcortical volume clusters were significantly related to CSF Aβ42 ($F = 8.30$, df1= 605, df2 = 3, pFDR < 0.001), p-tau ($F = 3.95$, df1 = 600, df2 = 3, pFDR = 0.01), and p-tau/Aβ42 ratio ($F = 10.40$, df1 = 601, df2 = 3, pFDR < 0.001). We also found significant positive associations between changes in thickness clusters and the p-tau/Aβ42 ratio ($F = 6.44$, df1 = 601, df2 = 3, pFDR < 0.001) and Aβ42 ($F = 7.08$, df1 = 605, df2 = 3, pFDR < 0.001). Changes in cortical area clusters were significantly related to CSF Aβ42 ($F = 4.54$, df1 = 605, df2 = 3, pFDR = 0.007). The ANOVA results were in the expected direction, with clusters displaying more brain decline showing lower Aβ42, higher p-

tau, and higher p-tau/Aβ42 ratio, and those showing relative brain maintenance exhibiting lower p-tau/Aβ42 ratio, and higher Aβ42. See **Supplementary Table 3**, **Figure 7** for the association with CSF AD biomarkers, and **Table 4** and **Supplementary Table 2** for the post-hoc comparisons across clusters, showing which specific subgroups had significantly different values.

Table 4 Associations between brain cluster assignment and CSF AD biomarkers at baseline

	CSF AD biomarkers bsl	(F [pFDR])	η^2 partial
Cluster change thickness	Aβ42	7.08 (< 0.001) [-a, c]	0.03
	p-tau	0.70 (0.62)	0.003
	p-tau/Aβ42 ratio	6.44 (< 0.001) [a, -c]	0.03
Cluster change area	Aβ42	4.54 (0.007) [-b, c]	0.02
	p-tau	0.16 (0.92)	8.29×10^{-4}
	p-tau/Aβ42 ratio	2.47 (0.08)	0.01
Cluster change subvolume	Aβ42	8.30 (< 0.001) [-a, c]	0.04
	p-tau	3.95 (0.01) [a]	0.02
	p-tau/Aβ42 ratio	10.40 (< 0.001) [a, -c, -d]	0.05

ANOVA models on the LME model outputs. Sex and mean age (and Aβ42 for p-tau change models) as covariates of no interest. Statistics represent F-values, pFDR corrected values, and

535 η^2 partial represents the effect size eta squared partial. The superscripts represent the significant
536 output ($p < 0.01$) of the post hoc multiple comparisons, where each cluster assignment is
537 compared against all: a) decline cluster > mean; b) mild decline > mean; c) mild maintenance
538 > mean; d) maintenance > mean. A negative sign indicates that the significant comparison was
539 lower than the mean.

540

541 **Figure 7 Significant associations between brain cluster assignment and AD CSF**
542 **biomarkers**

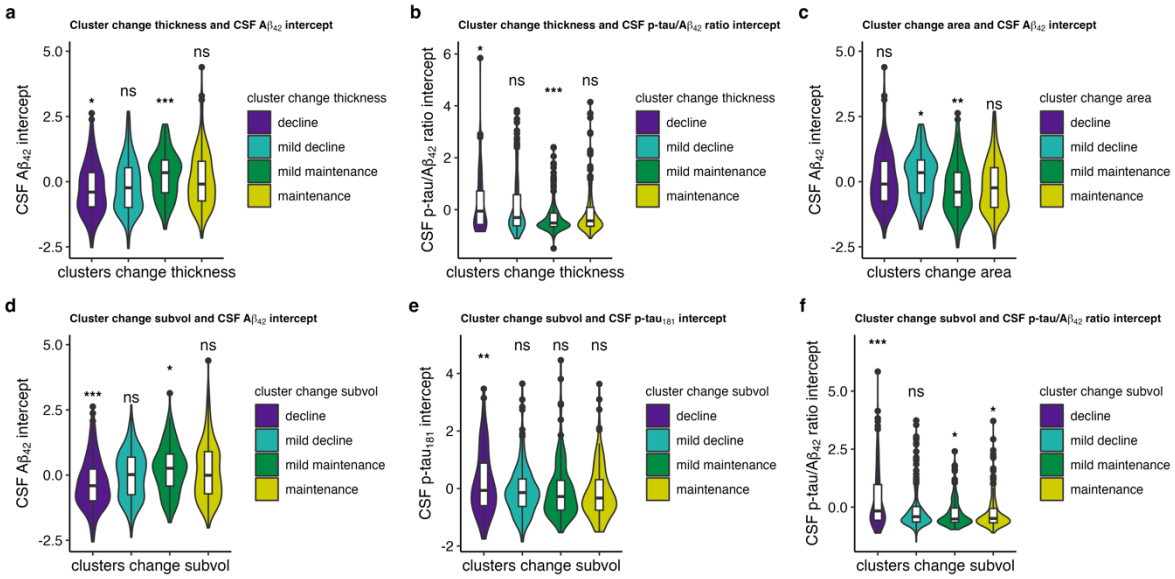

543

544 Post-hoc comparisons of means (one cluster vs all) for AD CSF biomarkers intercept. * = $p <$
545 0.05, ** = $p < 0.01$, *** = $p < 0.001$, ns = non-significant.

546

547 ## 3.6 Automated model selection for cognitive functioning and CSF core AD biomarkers

548 When using λ within 1 standard error of the minimum (the more conservative criterion), the
549 LASSO models dropped all the predictors. By selecting the less conservative criteria for
550 selecting λ (λ.min = 0.01), the optimal model for predicting the memory intercept included

551 only the cluster area change, which had nonzero coefficients. The best model predicting
552 memory change included the main effects of changes in thickness and subcortical volume, and
553 the interactions among the three brain features (λ.min = 0.003). The optimal model predicting
554 global cognition at baseline comprised thickness, area, and subcortical volume change main
555 effects (λ.min = 0.004), whereas global cognitive change included area and subcortical volume
556 main effects and their interactions (λ.min = 0.002). Regarding CSF AD biomarkers, we found
557 that the main effects of changes in thickness, area, and subcortical volume were associated with
558 CSF Aβ42 at baseline (λ.min = 0.01). Changes in subcortical volume best predicted p-tau
559 (λ.min = 0.01), whereas the main effects of changes in thickness and subcortical volume were
560 associated with the p-tau/Aβ42 ratio (λ.min = 0.01). See **Supplementary Table 4** for all the
561 stats.

562

563

564 ## 4. Discussion

565

566 We identified four ageotypes for cortical thickness, cortical area, and subcortical volume,
567 grouping participants based on the degree of morphometric change. The overlap across
568 modalities was low, indicating that a comprehensive understanding of structural brain changes
569 in aging requires the integration of different brain features. The analysis of the associations
570 between brain changes and cognitive function, as well as AD biomarkers, was beneficial in
571 comprehending the significance of these brain changes in normal aging. In particular,
572 clustering based on subcortical volumetric change was found to be highly sensitive to both
573 cognition and AD biomarkers. This suggests that ageotypes are relevant in understanding

574 cognitive decline in aging. Furthermore, the relationship with AD biomarkers indicates that
575 structural brain changes may give rise to an increased risk for later development of AD.

576

577 Clustering was strongly based on a main factor of decline, suggesting that differences in cluster
578 assignment could be attributed to a main "global" component of (modality-specific) brain
579 decline rather than to specific spatial patterns. This finding is consistent with a previous study
580 that used factor analysis on longitudinal volumetric ROIs changes and identified a general
581 factor of cortical volume change in aging (Cox et al., 2021) which accounted for 63% of the
582 longitudinal changes in the different regions. Similarly, Sele and colleagues (2020) found that
583 a component of decline (from PCA) accounted for approximately 35% of the longitudinal
584 volumetric change (slope differences) across different regions, especially temporal.

585

586 Although clusters were primarily determined by a global component of brain decline, some
587 regions were especially critical for cluster assignment. Specifically, we found that subtypes
588 based on both cortical thickness and cortical area change were strongly related to the degree of
589 bilateral decline in the temporal and inferior parietal regions. These regions are among those
590 suffering steeper age-related decline (Fjell et al., 2014b; Thambisetty et al., 2010), as well as
591 exhibiting higher inter-individual variability (Sele et al., 2020). Notable decline in these regions
592 can be seen also independently of *APOE* status and neurodegenerative processes reflected by
593 AD biomarkers Aβ42 and tau, and is often considered characteristic of normal aging
594 trajectories (Fjell et al., 2014a). Despite being highly vulnerable to aging, frontal regions did
595 not have a special influence in determining cluster assignment, with the exception of the
596 superior frontal cortex in cortical area change. One possible explanation is that despite showing
597 a steep decline, these regions also showed relatively low inter-individual variability in change.

598 In other words, older participants tended to show a similar degree of change in these regions
599 (Sele et al., 2021). Finally, we found that inter-individual variability in bilateral hippocampal
600 volume decline and enlargement of the lateral ventricles was relevant for identifying clusters
601 of subcortical volume changes. These regions are both strongly affected by age (Fjell et al.,
602 2014a; Takao et al., 2012) with a high degree of variability across individuals (Sele et al., 2021,
603 2020) and are also commonly affected by AD (Apostolova et al., 2012; Grundman et al., 2002;
604 Thompson et al., 2004).

605

606 Although individuals can be differentiated based on the main component of change within
607 modality, the different modalities provide largely independent information in the context of
608 age-related changes. A comprehensive approach that incorporates multiple measures of brain
609 morphometric changes is essential to understand structural brain changes in older age. Indeed,
610 there was minimal overlap in terms of cluster assignment among the brain features, particularly
611 for cortical thickness and area. These two measures of surface, which together define cortical
612 volume, are among other things thought to reflect the total number of cortical columns (area)
613 and the number of cells within a column (thickness) (Rakic, 1988), respectively. Both area and
614 thickness change are affected by increasing age, as shown by a cross-sectional and longitudinal
615 study (Hogstrom et al., 2013; Storsve et al., 2014), and show a constant negative relationship
616 across the adult lifespan (Storsve et al., 2014). Furthermore, these measures have distinct
617 contributions to the volumetric changes at different stages of life. During development, cortical
618 area changes play a significant role, and cortical thinning is the primary contributor in older
619 age (Walhovd et al., 2016). Nevertheless, they showed an opposite pattern within regions; that
620 is, those regions characterized by more thinning showed less decrease in area, and vice versa.
621 Sele and colleagues (2021) found both null and negative associations between cortical area and
622 cortical thickness change across individuals. Overall, these brain features show a unique

genetic signature (Panizzon et al., 2009), although recently other researchers have reported opposing effects on the impact of genetics on thickness and area (Grasby et al., 2020), and might display specific biological processes that may account for the varying contributions to age-related structural changes. Therefore, although individuals can be differentiated based on the main component of change within modality, the different modalities provide largely independent biological information in the context of age-related changes.

Our findings showed that participants displaying more thinning, more subcortical volume decline, and/or more cortical area loss showed worse global cognition at baseline. These results can be interpreted in two ways. First, integrating brain reserve (Katzman et al., 1988; Stern et al., 2019) and maintenance (Nyberg et al., 2012) frameworks together within the Matthew principle. The latter posits an interaction between variation in level and change to explain differences in brain and cognition; in other words, it suggests that individuals who begin with an advantage will accumulate and maintain more advantage over time, and vice versa. From this perspective, participants with higher cognition at baseline may have accumulated neural resources that allowed them to counterbalance the effect of age-related brain changes. Consequently, the more neural resources available at our starting point (brain reserve), which accumulate over time, the more the advantages over time, leading to maintenance of brain resources available in aging, which is translated into better cognitive performance in older age. However, education, one of the most popular proxies of cognitive reserve (Stern, 2012) used to explain individual differences in cognition, which correlates with higher cognition in aging, does not seem to have a meaningful impact on structural brain changes in aging (Nyberg et al., 2021), and does not affect the relationship between brain change and cognitive change (Lövdén et al., 2023), as would be predicted from the cognitive reserve account. Another alternative interpretation is that the relationship between global cognition and brain changes may capture

the ongoing changes in the brain and cognition that occur prior to, during, and maybe even after the follow-up period. In other words, the follow-up period can be viewed as a temporal "window" for observing slow trajectories of the brain and cognitive decline. Indeed, we found change in cortical surface area is related to both baseline cognition and cognitive change (as assessed by screening parameters). Further, even the screening tests used assess global cognition, they cannot be considered a pre-morbid cognitive assessment. Thus, brain change – baseline cognition relationships seem to reflect a dynamic sluggish association of paired cognitive and brain change. This might indicate that the global cognition factor captures changes that occurred prior to neuroimaging acquisition and cannot be accounted for by earlier factors. A recent paper (Walhovd et al., 2023) argues that the timing of lifespan influences is crucial to explain individual differences in brain and cognition. In fact, it appears that differences in the trajectories of change in brain and cognition can only partially explain the inter-individual variability in older age. Instead, individual differences may be largely attributed to early life factors that remain relatively stable over the adult lifespan.

Cortical area changes were significantly related to cognitive changes in contrast to cortical thickness. Cortical area typically may indicate the number of cortical columns and it is related to information-processing capacity, and this was observed in older adults who showed cortical area decline, as they also exhibited more decline in the global cognition factor over time. This finding is supported by other studies (Borgeest et al., 2021; Nyberg et al., 2023), although they used fluid cognition measures (assessed by a speed of processing test and Cattell Culture Fair test). Changes in cortical thickness may be likely due to dendritic atrophy, which occurs with increasing age, and late-onset lower cortical thickness is associated with cognitive decline (de Chastelaine et al., 2019). We speculate that we did not find any positive association between thinning and cognitive change within our temporal interval due to the inclusion of relatively

673 *young* older adults (aged 50 years and older). This may lead to relatively minor changes in
674 cortical thickness, which accelerate with higher age, especially after 60 years, as shown in a
675 previous study (Nyberg et al., 2023), where the association with cognitive change was
676 significant only at the final time point, when participants were older. As we can see, the time
677 interval is a critical factor in this context, and it is possible that both brain and cognitive changes
678 occur simultaneously in the same time frame, or, as we speculate in our case, cognitive changes
679 occur both prior to and later than our follow-up period. The global cognition factor, as
680 measured in our case by the MMSE and MOCA scores, appears to be an earlier and valid
681 predictor, capturing more general and systematic changes in the aging-disease continuum
682 compared to memory alone, which generally encompasses more specific and subtle changes.
683 Indeed, we did not observe any effect on memory. The relationship between MTL thinning and
684 hippocampal volume decline with memory changes is well established (Fjell et al., 2014b;
685 Gorbach et al., 2017; Leong et al., 2017). Hence, a possible explanation for this null association
686 might be due to the memory – brain associations being more regionally specific (e.g., medial
687 temporal lobe) than global cognitive scores.

688

689 Our results showed that more rapid cortical thinning, subcortical volume, and cortical area
690 decline over time were related to lower CSF Aβ42 levels at baseline. Previous studies have
691 reported conflicting results regarding the association between CSF Aβ42 and brain atrophy in
692 cognitively healthy older adults (Fjell et al., 2014a; Svenningsson et al., 2019; Tosun et al.,
693 2011; Wang et al., 2015). Indeed, some studies found that decreased Aβ42 levels were
694 associated with hippocampal loss but not cortical thinning in AD-signature regions (Pettigrew
695 et al., 2016; Wang et al., 2015). Conversely, another study (Arenaza-Urquijo et al., 2013) found
696 cortical thinning in AD-vulnerable regions, while another cross-sectional study found no
697 relationship between CSF Aβ42 positivity, hippocampal volume decline, or cortical thickness

(Svenningsson et al., 2019). A significant association between lower CSF Aβ42 and surface area decline has not previously been reported. In our study, change in each longitudinal brain feature was associated with Aβ42 . In addition, subcortical volumetric change was associated also to p-tau. Specifically, participants in the subcortical decline cluster, who showed higher p-tau and p-tau/Aβ42 ratio, as well as lower Aβ42 levels, may be at an increased risk for a subsequent clinical diagnosis of AD. Therefore, the association with AD biomarkers helps us understand the significance of these structural brain changes in the context of normal aging. Changes in the hippocampal volume and lateral ventricles are affected early in the disease process as long as AD biomarkers accumulate in the brain (Stricker et al., 2012). Overall, clustering of subcortical volume changes may provide helpful information for identifying individuals with an increased risk for a later clinical AD diagnosis, whereas the clustering of cortical features such as thickness and area may reflect different age-related brain processes.

4.1 Limitations and technical considerations

A strength of the present study is the use of longitudinal data for structural MRI, cognitive assessment, and CSF, which allows for a better capture of intra-individual changes over time. However, longitudinal studies can be affected by selective attrition, which means that results apply to the participants who did not drop out of the studies, who are known to be healthier, more educated, and with higher general cognitive ability than the general population (Beller et al., 2022; Salthouse, 2014). An additional problem with longitudinal data is the less than perfect reliability of the brain and cognitive change estimates. This aspect may help explain the stronger associations between brain change and baseline cognition compared to cognitive change. Additionally, it can be speculated that there is less variation in change than in level, making it more challenging to detect any systematic relationship. Another critical methodological aspect of this study is the merging of multiple cohorts, yielding increased

723 statistical power and reduced sampling bias compared to meta-analytical approaches. However,
724 this approach may also introduce new sources of error due to differences in measurements or
725 populations (Zuo et al., 2019). This decision leads to the use of different memory and global
726 cognitive tests across the different cohorts, and may lead to small biases because the same
727 underlying construct is not necessarily captured.

728

729

730 ## 5. Conclusions

731

732 In summary, this study identified four distinct ageotypes based on the global pattern of brain
733 changes within cortical thickness, cortical area and subcortical volume measures over time.
734 The minimal overlap across modalities highlights the need to combine all the features to better
735 capture and understand age-related brain changes. Furthermore, the clustering of regional brain
736 changes proved to be a valuable tool for explaining cognitive and biomarker differences in
737 cognitively unimpaired older adults.

Declaration of interest

HZ has served at scientific advisory boards and/or as a consultant for Abbvie, Acumen, Alector, Alzinova, ALZPath, Amylyx, Annexon, Apellis, Artery Therapeutics, AZTherapies, Cognito Therapeutics, CogRx, Denali, Eisai, Merry Life, Nervgen, Novo Nordisk, Optoceutics, Passage Bio, Pinteon Therapeutics, Prothena, Red Abbey Labs, reMYND, Roche, Samumed, Siemens Healthineers, Triplet Therapeutics, and Wave, has given lectures in symposia sponsored by Alzecure, Biogen, Cellectricon, Fujirebio, Lilly, Novo Nordisk, and Roche, and is a co-founder of Brain Biomarker Solutions in Gothenburg AB (BBS), which is a part of the GU Ventures Incubator Program (outside submitted work). KB has served as a consultant and at advisory boards for AC Immune, Acumen, ALZPath, AriBio, BioArctic, Biogen, Eisai, Lilly, Moleac Pte. Ltd, Novartis, Ono Pharma, Prothena, Roche Diagnostics, and Siemens Healthineers; has served at data monitoring committees for Julius Clinical and Novartis; has given lectures, produced educational materials and participated in educational programs for AC Immune, Biogen, Celdara Medical, Eisai and Roche Diagnostics; and is a co-founder of Brain Biomarker Solutions in Gothenburg AB (BBS), which is a part of the GU Ventures Incubator Program, outside the work presented in this paper. All conflicts of interest are unrelated to the work presented in this paper. The remaining authors declare no competing interests.

Funding and acknowledgements

This work was supported by the Department of Psychology, University of Oslo (to K.B.W., A.M.F.), the Norwegian Research Council (to K.B.W., A.M.F., D.V.P [ES694407]) and the

762 project has received funding from the European Research Council's Starting Grant scheme
763 under grant agreements 283634, 725025 (to A.M.F.). HZ is a Wallenberg Scholar and a
764 Distinguished Professor at the Swedish Research Council supported by grants from the
765 Swedish Research Council (#2023-00356; #2022-01018 and #2019-02397), the European
766 Union's Horizon Europe research and innovation programme under grant agreement No
767 101053962, Swedish State Support for Clinical Research (#ALFGBG-71320), the Alzheimer
768 Drug Discovery Foundation (ADDF), USA (#201809-2016862), the AD Strategic Fund and
769 the Alzheimer's Association (#ADSF-21-831376-C, #ADSF-21-831381-C, #ADSF-21-
770 831377-C, and #ADSF-24-1284328-C), the Bluefield Project, Cure Alzheimer's Fund, the
771 Olav Thon Foundation, the Erling-Persson Family Foundation, Stiftelsen för Gamla
772 Tjänarinnor, Hjärnfonden, Sweden (#FO2022-0270), the European Union's Horizon 2020
773 research and innovation programme under the Marie Skłodowska-Curie grant agreement No
774 860197 (MIRIADE), the European Union Joint Programme – Neurodegenerative Disease
775 Research (JPND2021-00694), the National Institute for Health and Care Research University
776 College London Hospitals Biomedical Research Centre, and the UK Dementia Research
777 Institute at UCL (UKDRI-1003). KB is supported by the Swedish Research Council (2017-
778 00915 and 2022-00732), the Alzheimer Drug Discovery Foundation (ADDF), USA (RDAPB-
779 201809-2016615), the Swedish Alzheimer Foundation (AF-930351, AF-939721 and AF-
780 968270), Hjärnfonden, Sweden (FO2017-0243 and ALZ2022-0006) the Swedish state under
781 the agreement between the Swedish government and the County Councils, the ALF-agreement
782 (ALFGBG-715986 and ALFGBG-965240), the European Union Joint Program for
783 Neurodegenerative Disorders (JPND2019-466-236), the National Institute of Health (NIH),
784 USA, (grant 1R01AG068398-01), and the Alzheimer's Association 2021 Zenith Award (ZEN-
785 21-848495) and the Alzheimer's Association 2022-2025 Grant (SG-23-1038904 QC). L.O.W.
786 and data collection in COGNORM is funded by the South-Eastern Norway Regional Health

Authorities (#2017095) The Norwegian Health Association (#19536) and by Wellcome Leap's Dynamic Resilience Program (jointly funded by Temasek Trust) #104617). The funding sources had no role in the study design. Data collection and sharing for this project were funded by the ADNI (NIH Grant U01 AG024904) and DOD ADNI (Department of Defense award number W81XWH-12-2-0012). ADNI is funded by the National Institute on Aging, the National Institute of Biomedical Imaging and Bioengineering, and through generous contributions from the following: AbbVie, Alzheimer's Association; Alzheimer's Drug Discovery Foundation; Araclon Biotech; BioClinica, Inc.; Biogen; Bristol-Myers Squibb Company; CereSpir, Inc.; Cogstate Eisai Inc.; Elan Pharmaceuticals, Inc.; Eli Lilly and Company; EuroImmun; F. Hoffmann-La Roche Ltd and its affiliated company Genentech, Inc.; Fujirebio; GE Healthcare; IXICO Ltd.; Janssen Alzheimer Immunotherapy Research & Development, LLC.; Johnson & Johnson Pharmaceutical Research & Development LLC.; Lumosity; Lundbeck; Merck & Co., Inc.; Meso Scale Diagnostics, LLC.; NeuroRx Research; Neurotrack Technologies; Novartis Pharmaceuticals Corporation; Pfizer Inc.; Piramal Imaging; Servier; Takeda Pharmaceutical Company; and Transition Therapeutics. The Canadian Institutes of Health Research is providing funds to support ADNI clinical sites in Canada. Private sector contributions are facilitated by the Foundation for the National Institutes of Health (http://www.fnih.org). The grantee organization is the Northern California Institute for Research and Education, and the study is coordinated by the Alzheimer's Therapeutic Research Institute at the University of Southern California. ADNI data are disseminated by the Laboratory for Neuro Imaging at the University of Southern California. The investigators within the ADNI contributed to the design and implementation of ADNI and/or provided data but did not participate in analysis or writing of this report. A complete listing of ADNI investigators can be found at: http://adni.loni.usc.edu/wp-content/uploads/how_to_apply/ADNI_Acknowledgement_List.pdf. OASIS 3 data were

812 provided [in part] by OASIS 3: Longitudinal Multimodal Neuroimaging: Principal
813 Investigators: T. Benzinger, D. Marcus, J. Morris; NIH P30 AG066444, P50 AG00561, P30
814 NS09857781, P01 AG026276, P01 AG003991, R01 AG043434, UL1 TR000448, R01
815 EB009352. AV-45 doses were provided by Avid Radiopharmaceuticals, a wholly owned
816 subsidiary of Eli Lilly. Some of the data used in preparation of this article were obtained from
817 the PREVENT-AD program (Breitner et al., 2016). PREVENT-AD was funded by the
818 Canadian Institutes of Health Research, McGill University, the Fonds de Recherche du Québec
819 – Santé, Alzheimer's Association, Brain Canada, the Government of Canada, the Canada Fund
820 for Innovation, the Douglas Hospital Research Centre and Foundation, the Levesque
821 Foundation, an unrestricted research grant from Pfizer Canada. Some of the data used in the
822 preparation of this article was obtained from the AIBL. AIBL is funded by the Commonwealth
823 Scientific and Industrial Research Organisation (CSIRO), which was made available at the
824 ADNI database (www.loni.usc.edu/ADNI). The AIBL researchers contributed data but did not
825 participate in analysis or writing of this report. AIBL researchers are listed at
826 www.aibl.csiro.au. Some of the data used in the preparation of this article were obtained from
827 the Harvard Aging Brain Study (HABS - P01AG036694; https://habs.mgh.harvard.edu).
828 HABS data release 2.0, obtained August, 2022 via habs.mgh.harvard.edu. The HABS study
829 was launched in 2010, funded by the National Institute on Aging, and is led by principal
830 investigators Reisa A. Sperling MD and Keith A. Johnson MD at Massachusetts General
831 Hospital/Harvard Medical School in Boston, MA.

832

833

834

References

Ahadi, S., Zhou, W., Schüssler-Fiorenza Rose, S.M., Sailani, M.R., Contrepois, K., Avina, M., Ashland, M., Brunet, A., Snyder, M., 2020. Personal aging markers and ageotypes revealed by deep longitudinal profiling. Nat. Med. 26, 83–90. https://doi.org/10.1038/s41591-019-0719-5

Apostolova, L.G., Green, A.E., Babakchanian, S., Hwang, K.S., Chou, Y.-Y., Toga, A.W., Thompson, P.M., 2012. Hippocampal atrophy and ventricular enlargement in normal aging, mild cognitive impairment and Alzheimer's disease. Alzheimer Dis. Assoc. Disord. 26, 17–27. https://doi.org/10.1097/WAD.0b013e3182163b62

Arenaza-Urquijo, E.M., Molinuevo, J.-L., Sala-Llonch, R., Solé-Padullés, C., Balasa, M., Bosch, B., Olives, J., Antonell, A., Lladó, A., Sánchez-Valle, R., Rami, L., Bartrés-Faz, D., 2013. Cognitive Reserve Proxies Relate to Gray Matter Loss in Cognitively Healthy Elderly with Abnormal Cerebrospinal Fluid Amyloid-β Levels. J. Alzheimers Dis. 35, 715–726. https://doi.org/10.3233/JAD-121906

Bates, D., Mächler, M., Bolker, B., Walker, S., 2015. Fitting Linear Mixed-Effects Models Using lme4. J. Stat. Softw. 67, 1–48. https://doi.org/10.18637/jss.v067.i01

Beasley, T.M., Schumacker, R.E., 1995. Multiple Regression Approach to Analyzing Contingency Tables: Post Hoc and Planned Comparison Procedures. J. Exp. Educ. 64, 79–93.

Beller, J., Geyer, S., Epping, J., 2022. Health and study dropout: health aspects differentially predict attrition. BMC Med. Res. Methodol. 22, 31. https://doi.org/10.1186/s12874-022-01508-w

858 Benjamini, Y., Hochberg, Y., 1995. Controlling the False Discovery Rate: A Practical and
859 Powerful Approach to Multiple Testing. J. R. Stat. Soc. Ser. B Methodol. 57, 289–300.
860 https://doi.org/10.1111/j.2517-6161.1995.tb02031.x
861 Borgeest, G.S., Henson, R.N., Kietzmann, T.C., Madan, C.R., Fox, T., Malpetti, M.,
862 Fuhrmann, D., Knights, E., Carlin, J.D., Cam-CAN, Kievit, R.A., 2021. A
863 morphometric double dissociation: cortical thickness is more related to aging; surface
864 area is more related to cognition. https://doi.org/10.1101/2021.09.30.462545
865 Breitner, J.C.S., Poirier, J., Etienne, P.E., Leoutsakos, J.M., 2016. Rationale and Structure for
866 a New Center for Studies on Prevention of Alzheimer's Disease (StoP-AD). J. Prev.
867 Alzheimers Dis. 3, 236–242. https://doi.org/10.14283/jpad.2016.121
868 Buuren, S. van, Groothuis-Oudshoorn, K., 2011. mice: Multivariate Imputation by Chained
869 Equations in R. J. Stat. Softw. 45, 1–67. https://doi.org/10.18637/jss.v045.i03
870 Capogna, E., Sneve, M.H., Raud, L., Folvik, L., Ness, H.T., Walhovd, K.B., Fjell, A.M., Vidal-
871 Piñeiro, D., 2023a. Whole-brain connectivity during encoding: age-related differences
872 and associations with cognitive and brain structural decline. Cereb. Cortex 33, 68–82.
873 https://doi.org/10.1093/cercor/bhac053
874 Capogna, E., Watne, L.O., Sørensen, Ø., Guichelaar, C.J., Idland, A.V., Halaas, N.B.,
875 Blennow, K., Zetterberg, H., Walhovd, K.B., Fjell, A.M., Vidal-Piñeiro, D., 2023b.
876 Associations of neuroinflammatory IL-6 and IL-8 with brain atrophy, memory decline,
877 and core AD biomarkers – in cognitively unimpaired older adults. Brain. Behav.
878 Immun. 113, 56–65. https://doi.org/10.1016/j.bbi.2023.06.027
879 Clark, L.R., Berman, S.E., Norton, D., Koscik, R.L., Jonaitis, E., Blennow, K., Bendlin, B.B.,
880 Asthana, S., Johnson, S.C., Zetterberg, H., Carlsson, C.M., 2018. Age-accelerated
881 cognitive decline in asymptomatic adults with CSF β-amyloid. Neurology 90, e1306–
882 e1315. https://doi.org/10.1212/WNL.0000000000005291

883 Cox, S.R., Harris, M.A., Ritchie, S.J., Buchanan, C.R., Valdés Hernández, M.C., Corley, J.,
884 Taylor, A.M., Madole, J.W., Harris, S.E., Whalley, H.C., McIntosh, A.M., Russ, T.C.,
885 Bastin, M.E., Wardlaw, J.M., Deary, I.J., Tucker-Drob, E.M., 2021. Three major
886 dimensions of human brain cortical ageing in relation to cognitive decline across the
887 eighth decade of life. Mol. Psychiatry 26, 2651–2662. https://doi.org/10.1038/s41380-
888 020-00975-1
889 Crane, P.K., Carle, A., Gibbons, L.E., Insel, P., Mackin, R.S., Gross, A., Jones, R.N.,
890 Mukherjee, S., Curtis, S.M., Harvey, D., Weiner, M., Mungas, D., 2012. Development
891 and assessment of a composite score for memory in the Alzheimer's Disease
892 Neuroimaging Initiative (ADNI). Brain Imaging Behav. 6, 502–516.
893 https://doi.org/10.1007/s11682-012-9186-z
894 Dagley, A., LaPoint, M., Huijbers, W., Hedden, T., McLaren, D.G., Chatwal, J.P., Papp, K.V.,
895 Amariglio, R.E., Blacker, D., Rentz, D.M., Johnson, K.A., Sperling, R.A., Schultz,
896 A.P., 2017. Harvard Aging Brain Study: Dataset and accessibility. NeuroImage, Data
897 Sharing Part II 144, 255–258. https://doi.org/10.1016/j.neuroimage.2015.03.069
898 Dale, A.M., Fischl, B., Sereno, M.I., 1999. Cortical surface-based analysis. I. Segmentation
899 and surface reconstruction. NeuroImage 9, 179–194.
900 https://doi.org/10.1006/nimg.1998.0395
901 de Chastelaine, M., Donley, B.E., Kennedy, K.M., Rugg, M.D., 2019. Age moderates the
902 relationship between cortical thickness and cognitive performance. Neuropsychologia
903 132, 107136. https://doi.org/10.1016/j.neuropsychologia.2019.107136
904 Delis, D.C., Kramer, J.H., Kaplan, E., Ober, B.A., 2000. Manual for the California verbal
905 learning test,(CVLT-II). San Antonio TX Psychol. Corp.

906 Destrieux, C., Fischl, B., Dale, A., Halgren, E., 2010. Automatic parcellation of human cortical
907 gyri and sulci using standard anatomical nomenclature. NeuroImage 53, 1–15.
908 https://doi.org/10.1016/j.neuroimage.2010.06.010
909 Ellis, K.A., Bush, A.I., Darby, D., De Fazio, D., Foster, J., Hudson, P., Lautenschlager, N.T.,
910 Lenzo, N., Martins, R.N., Maruff, P., Masters, C., Milner, A., Pike, K., Rowe, C.,
911 Savage, G., Szoeke, C., Taddei, K., Villemagne, V., Woodward, M., Ames, D., AIBL
912 Research Group, 2009. The Australian Imaging, Biomarkers and Lifestyle (AIBL)
913 study of aging: methodology and baseline characteristics of 1112 individuals recruited
914 for a longitudinal study of Alzheimer's disease. Int. Psychogeriatr. 21, 672–687.
915 https://doi.org/10.1017/S1041610209009405
916 Fischl, B., Salat, D.H., Busa, E., Albert, M., Dieterich, M., Haselgrove, C., van der Kouwe, A.,
917 Killiany, R., Kennedy, D., Klaveness, S., Montillo, A., Makris, N., Rosen, B., Dale,
918 A.M., 2002. Whole Brain Segmentation. Neuron 33, 341–355.
919 https://doi.org/10.1016/S0896-6273(02)00569-X
920 Fischl, B., Sereno, M.I., Dale, A.M., 1999. Cortical surface-based analysis. II: Inflation,
921 flattening, and a surface-based coordinate system. NeuroImage 9, 195–207.
922 https://doi.org/10.1006/nimg.1998.0396
923 Fjell, A.M., McEvoy, L., Holland, D., Dale, A.M., Walhovd, K.B., 2014a. What is normal in
924 normal aging? Effects of aging, amyloid and Alzheimer's disease on the cerebral cortex
925 and the hippocampus. Prog. Neurobiol. 117, 20–40.
926 https://doi.org/10.1016/j.pneurobio.2014.02.004
927 Fjell, A.M., Sørensen, Ø., Wang, Y., Amlien, I.K., Baaré, W.F.C., Bartrés-Faz, D., Bertram,
928 L., Boraxbekk, C.-J., Brandmaier, A.M., Demuth, I., Drevon, C.A., Ebmeier, K.P.,
929 Ghisletta, P., Kievit, R., Kühn, S., Skak Madsen, K., Mowinckel, A.M., Nyberg, L.,
930 Sexton, C.E., Solé-Padullés, C., Vidal-Piñeiro, D., Wagner, G., Watne, L.O., Walhovd,

K.B., 2023. Sleep duration and brain atrophy – phenotypic associations and genotypic covariance. Nat. Hum. Behav.

Fjell, A.M., Walhovd, K.B., 2010. Structural brain changes in aging: courses, causes and cognitive consequences. Rev. Neurosci. 21, 187–221. https://doi.org/10.1515/revneuro.2010.21.3.187

Fjell, A.M., Walhovd, K.B., Fennema-Notestine, C., McEvoy, L.K., Hagler, D.J., Holland, D., Brewer, J.B., Dale, A.M., Initiative, for the A.D.N., 2010. CSF Biomarkers in Prediction of Cerebral and Clinical Change in Mild Cognitive Impairment and Alzheimer's Disease. J. Neurosci. 30, 2088–2101. https://doi.org/10.1523/JNEUROSCI.3785-09.2010

Fjell, A.M., Westlye, L.T., Grydeland, H., Amlien, I., Espeseth, T., Reinvang, I., Raz, N., Dale, A.M., Walhovd, K.B., for the Alzheimer Disease Neuroimaging Initiative, 2014b. Accelerating Cortical Thinning: Unique to Dementia or Universal in Aging? Cereb. Cortex 24, 919–934. https://doi.org/10.1093/cercor/bhs379

Folstein, M.F., Folstein, S.E., McHugh, P.R., 1975. "Mini-mental state". A practical method for grading the cognitive state of patients for the clinician. J. Psychiatr. Res. 12, 189–198. https://doi.org/10.1016/0022-3956(75)90026-6

Garcia-Diaz, A.I., Segura, B., Baggio, H.C., Marti, M.J., Valldeoriola, F., Compta, Y., Vendrell, P., Bargallo, N., Tolosa, E., Junque, C., 2014. Structural MRI correlates of the MMSE and pentagon copying test in Parkinson's disease. Parkinsonism Relat. Disord. 20, 1405–1410. https://doi.org/10.1016/j.parkreldis.2014.10.014

Gorbach, T., Pudas, S., Bartrés-Faz, D., Brandmaier, A.M., Düzel, S., Henson, R.N., Idland, A.-V., Lindenberger, U., Macià Bros, D., Mowinckel, A.M., Solé-Padullés, C., Sørensen, Ø., Walhovd, K.B., Watne, L.O., Westerhausen, R., Fjell, A.M., Nyberg, L., 2020. Longitudinal association between hippocampus atrophy and episodic-memory

956 decline in non-demented APOE ε4 carriers. Alzheimers Dement. Diagn. Assess. Dis.
957 Monit. 12, e12110. https://doi.org/10.1002/dad2.12110
958 Gorbach, T., Pudas, S., Lundquist, A., Orädd, G., Josefsson, M., Salami, A., de Luna, X.,
959 Nyberg, L., 2017. Longitudinal association between hippocampus atrophy and
960 episodic-memory decline. Neurobiol. Aging 51, 167–176.
961 https://doi.org/10.1016/j.neurobiolaging.2016.12.002
962 Gorgolewski, K.J., Auer, T., Calhoun, V.D., Craddock, R.C., Das, S., Duff, E.P., Flandin, G.,
963 Ghosh, S.S., Glatard, T., Halchenko, Y.O., Handwerker, D.A., Hanke, M., Keator, D.,
964 Li, X., Michael, Z., Maumet, C., Nichols, B.N., Nichols, T.E., Pellman, J., Poline, J.-
965 B., Rokem, A., Schaefer, G., Sochat, V., Triplett, W., Turner, J.A., Varoquaux, G.,
966 Poldrack, R.A., 2016. The brain imaging data structure, a format for organizing and
967 describing outputs of neuroimaging experiments. Sci. Data 3, 160044.
968 https://doi.org/10.1038/sdata.2016.44
969 Grasby, K.L., Jahanshad, N., Painter, J.N., Colodro-Conde, L., Bralten, J., Hibar, D.P., Lind,
970 P.A., Pizzagalli, F., Ching, C.R.K., McMahon, M.A.B., Shatokhina, N., Zsembik,
971 L.C.P., Thomopoulos, S.I., Zhu, A.H., Strike, L.T., Agartz, I., Alhusaini, S., Almeida,
972 M.A.A., Alnæs, D., Amlien, I.K., Andersson, M., Ard, T., Armstrong, N.J., Ashley-
973 Koch, A., Atkins, J.R., Bernard, M., Brouwer, R.M., Buimer, E.E.L., Bülow, R.,
974 Bürger, C., Cannon, D.M., Chakravarty, M., Chen, Q., Cheung, J.W., Couvy-Duchesne,
975 B., Dale, A.M., Dalvie, S., de Araujo, T.K., de Zubicaray, G.I., de Zwarte, S.M.C., den
976 Braber, A., Doan, N.T., Dohm, K., Ehrlich, S., Engelbrecht, H.-R., Erk, S., Fan, C.C.,
977 Fedko, I.O., Foley, S.F., Ford, J.M., Fukunaga, M., Garrett, M.E., Ge, T., Giddaluru,
978 S., Goldman, A.L., Green, M.J., Groenewold, N.A., Grotegerd, D., Gurholt, T.P.,
979 Gutman, B.A., Hansell, N.K., Harris, M.A., Harrison, M.B., Haswell, C.C., Hauser, M.,
980 Herms, S., Heslenfeld, D.J., Ho, N.F., Hoehn, D., Hoffmann, P., Holleran, L.,

Hoogman, M., Hottenga, J.-J., Ikeda, M., Janowitz, D., Jansen, I.E., Jia, T., Jockwitz, C., Kanai, R., Karama, S., Kasperaviciute, D., Kaufmann, T., Kelly, S., Kikuchi, M., Klein, M., Knapp, M., Knodt, A.R., Krämer, B., Lam, M., Lancaster, T.M., Lee, P.H., Lett, T.A., Lewis, L.B., Lopes-Cendes, I., Luciano, M., Macciardi, F., Marquand, A.F., Mathias, S.R., Melzer, T.R., Milaneschi, Y., Mirza-Schreiber, N., Moreira, J.C.V., Mühleisen, T.W., Müller-Myhsok, B., Najt, P., Nakahara, S., Nho, K., Olde Loohuis, L.M., Orfanos, D.P., Pearson, J.F., Pitcher, T.L., Pütz, B., Quidé, Y., Ragothaman, A., Rashid, F.M., Reay, W.R., Redlich, R., Reinbold, C.S., Repple, J., Richard, G., Riedel, B.C., Risacher, S.L., Rocha, C.S., Mota, N.R., Salminen, L., Saremi, A., Saykin, A.J., Schlag, F., Schmaal, L., Schofield, P.R., Secolin, R., Shapland, C.Y., Shen, L., Shin, J., Shumskaya, E., Sønderby, I.E., Sprooten, E., Tansey, K.E., Teumer, A., Thalamuthu, A., Tordesillas-Gutiérrez, D., Turner, J.A., Uhlmann, A., Vallerga, C.L., van der Meer, D., van Donkelaar, M.M.J., van Eijk, L., van Erp, T.G.M., van Haren, N.E.M., van Rooij, D., van Tol, M.-J., Veldink, J.H., Verhoef, E., Walton, E., Wang, M., Wang, Y., Wardlaw, J.M., Wen, W., Westlye, L.T., Whelan, C.D., Witt, S.H., Wittfeld, K., Wolf, C., Wolfers, T., Wu, J.Q., Yasuda, C.L., Zaremba, D., Zhang, Z., Zwiers, M.P., Artiges, E., Assareh, A.A., Ayesa-Arriola, R., Belger, A., Brandt, C.L., Brown, G.G., Cichon, S., Curran, J.E., Davies, G.E., Degenhardt, F., Dennis, M.F., Dietsche, B., Djurovic, S., Doherty, C.P., Espiritu, R., Garijo, D., Gil, Y., Gowland, P.A., Green, R.C., Häusler, A.N., Heindel, W., Ho, B.-C., Hoffmann, W.U., Holsboer, F., Homuth, G., Hosten, N., Jack, C.R., Jang, M., Jansen, A., Kimbrel, N.A., Kolskår, K., Koops, S., Krug, A., Lim, K.O., Luykx, J.J., Mathalon, D.H., Mather, K.A., Mattay, V.S., Matthews, S., Mayoral Van Son, J., McEwen, S.C., Melle, I., Morris, D.W., Mueller, B.A., Nauck, M., Nordvik, J.E., Nöthen, M.M., O'Leary, D.S., Opel, N., Martinot, M.-L.P., Pike, G.B., Preda, A., Quinlan, E.B., Rasser, P.E., Ratnakar, V., Reppermund, S., Steen, V.M.,

1006 Tooney, P.A., Torres, F.R., Veltman, D.J., Voyvodic, J.T., Whelan, R., White, T.,
1007 Yamamori, H., Adams, H.H.H., Bis, J.C., Debette, S., Decarli, C., Fornage, M.,
1008 Gudnason, V., Hofer, E., Ikram, M.A., Launer, L., Longstreth, W.T., Lopez, O.L.,
1009 Mazoyer, B., Mosley, T.H., Roshchupkin, G.V., Satizabal, C.L., Schmidt, R., Seshadri,
1010 S., Yang, Q., Alzheimer's Disease Neuroimaging Initiative, CHARGE Consortium,
1011 EPIGEN Consortium, IMAGEN Consortium, SYS Consortium, Parkinson's
1012 Progression Markers Initiative, Alvim, M.K.M., Ames, D., Anderson, T.J., Andreassen,
1013 O.A., Arias-Vasquez, A., Bastin, M.E., Baune, B.T., Beckham, J.C., Blangero, J.,
1014 Boomsma, D.I., Brodaty, H., Brunner, H.G., Buckner, R.L., Buitelaar, J.K., Bustillo,
1015 J.R., Cahn, W., Cairns, M.J., Calhoun, V., Carr, V.J., Caseras, X., Caspers, S.,
1016 Cavalleri, G.L., Cendes, F., Corvin, A., Crespo-Facorro, B., Dalrymple-Alford, J.C.,
1017 Dannlowski, U., de Geus, E.J.C., Deary, I.J., Delanty, N., Depondt, C., Desrivières, S.,
1018 Donohoe, G., Espeseth, T., Fernández, G., Fisher, S.E., Flor, H., Forstner, A.J., Francks,
1019 C., Franke, B., Glahn, D.C., Gollub, R.L., Grabe, H.J., Gruber, O., Håberg, A.K., Hariri,
1020 A.R., Hartman, C.A., Hashimoto, R., Heinz, A., Henskens, F.A., Hillegers, M.H.J.,
1021 Hoekstra, P.J., Holmes, A.J., Hong, L.E., Hopkins, W.D., Hulshoff Pol, H.E., Jernigan,
1022 T.L., Jönsson, E.G., Kahn, R.S., Kennedy, M.A., Kircher, T.T.J., Kochunov, P., Kwok,
1023 J.B.J., Le Hellard, S., Loughland, C.M., Martin, N.G., Martinot, J.-L., McDonald, C.,
1024 McMahon, K.L., Meyer-Lindenberg, A., Michie, P.T., Morey, R.A., Mowry, B.,
1025 Nyberg, L., Oosterlaan, J., Ophoff, R.A., Pantelis, C., Paus, T., Pausova, Z., Penninx,
1026 B.W.J.H., Polderman, T.J.C., Posthuma, D., Rietschel, M., Roffman, J.L., Rowland,
1027 L.M., Sachdev, P.S., Sämann, P.G., Schall, U., Schumann, G., Scott, R.J., Sim, K.,
1028 Sisodiya, S.M., Smoller, J.W., Sommer, I.E., St Pourcain, B., Stein, D.J., Toga, A.W.,
1029 Trollor, J.N., Van der Wee, N.J.A., van 't Ent, D., Völzke, H., Walter, H., Weber, B.,
1030 Weinberger, D.R., Wright, M.J., Zhou, J., Stein, J.L., Thompson, P.M., Medland, S.E.,

ENHANCING NEUROIMAGING GENETICS THROUGH META-ANALYSIS CONSORTIUM (ENIGMA)—GENETICS WORKING GROUP, 2020. The genetic architecture of the human cerebral cortex. Science 367, eaay6690. https://doi.org/10.1126/science.aay6690

Grundman, M., Sencakova, D., Jack, C.R., Petersen, R.C., Kim, H.T., Schultz, A., Weiner, M.F., DeCarli, C., DeKosky, S.T., van Dyck, C., Thomas, R.G., Thal, L.J., the Alzheimer's Disease Cooperative Study, 2002. Brain MRI hippocampal volume and prediction of clinical status in a mild cognitive impairment trial. J. Mol. Neurosci. 19, 23–27. https://doi.org/10.1007/s12031-002-0006-6

Hedden, T., Oh, H., Younger, A.P., Patel, T.A., 2013. Meta-analysis of amyloid-cognition relations in cognitively normal older adults. Neurology 80, 1341–1348. https://doi.org/10.1212/WNL.0b013e31828ab35d

Hogstrom, L.J., Westlye, L.T., Walhovd, K.B., Fjell, A.M., 2013. The structure of the cerebral cortex across adult life: age-related patterns of surface area, thickness, and gyrification. Cereb. Cortex N. Y. N 1991 23, 2521–2530. https://doi.org/10.1093/cercor/bhs231

Idland, A.-V., Sala-Llonch, R., Borza, T., Watne, L.O., Wyller, T.B., Brækhus, A., Zetterberg, H., Blennow, K., Walhovd, K.B., Fjell, A.M., 2017. CSF neurofilament light levels predict hippocampal atrophy in cognitively healthy older adults. Neurobiol. Aging 49, 138–144. https://doi.org/10.1016/j.neurobiolaging.2016.09.012

Jack, C.R., Bennett, D.A., Blennow, K., Carrillo, M.C., Dunn, B., Haeberlein, S.B., Holtzman, D.M., Jagust, W., Jessen, F., Karlawish, J., Liu, E., Molinuevo, J.L., Montine, T., Phelps, C., Rankin, K.P., Rowe, C.C., Scheltens, P., Siemers, E., Snyder, H.M., Sperling, R., Contributors, 2018. NIA-AA Research Framework: Toward a biological definition of Alzheimer's disease. Alzheimers Dement. J. Alzheimers Assoc. 14, 535–562. https://doi.org/10.1016/j.jalz.2018.02.018

John, C.R., Watson, D., Russ, D., Goldmann, K., Ehrenstein, M., Pitzalis, C., Lewis, M., Barnes, M., 2020. M3C: Monte Carlo reference-based consensus clustering. Sci. Rep. 10, 1816. https://doi.org/10.1038/s41598-020-58766-1

Josefsson, M., de Luna, X., Pudas, S., Nilsson, L.-G., Nyberg, L., 2012. Genetic and Lifestyle Predictors of 15-Year Longitudinal Change in Episodic Memory. J. Am. Geriatr. Soc. 60, 2308–2312. https://doi.org/10.1111/jgs.12000

Katzman, R., Terry, R., DeTeresa, R., Brown, T., Davies, P., Fuld, P., Renbing, X., Peck, A., 1988. Clinical, pathological, and neurochemical changes in dementia: A subgroup with preserved mental status and numerous neocortical plaques. Ann. Neurol. 23, 138–144. https://doi.org/10.1002/ana.410230206

LaMontagne, P., Benzinger, T. LS., Morris, J. C., Keefe, S., Hornbeck, Russ., Xiong, C., Grant, E., Hassenstab, J., Moulder, K., Vlassenko, A. G., Raichle, M. E., Cruchaga, C., Marcus, D., 2019. OASIS-3: Longitudinal Neuroimaging, Clinical, and Cognitive Dataset for Normal Aging and Alzheimer Disease. medRxiv 2019.12.13.19014902. https://doi.org/10.1101/2019.12.13.19014902

Landis, J.R., Koch, G.G., 1977. The Measurement of Observer Agreement for Categorical Data. Biometrics 33, 159–174. https://doi.org/10.2307/2529310

Lemaitre, H., Goldman, A.L., Sambataro, F., Verchinski, B.A., Meyer-Lindenberg, A., Weinberger, D.R., Mattay, V.S., 2012. Normal age-related brain morphometric changes: nonuniformity across cortical thickness, surface area and gray matter volume? Neurobiol. Aging 33, 617.e1–9. https://doi.org/10.1016/j.neurobiolaging.2010.07.013

Leong, R.L.F., Lo, J.C., Sim, S.K.Y., Zheng, H., Tandi, J., Zhou, J., Chee, M.W.L., 2017. Longitudinal brain structure and cognitive changes over 8 years in an East Asian cohort. NeuroImage 147, 852–860. https://doi.org/10.1016/j.neuroimage.2016.10.016

1080 Lindenberger, U., 2014. Human cognitive aging: corriger la fortune? Science 346, 572–578.
1081 https://doi.org/10.1126/science.1254403
1082 Lövdén, M., Pagin, A., Bartrés-Faz, D., Boraxbekk, C.-J., Brandmaier, A.M., Demnitz, N.,
1083 Drevon, C.A., Ebmeier, K.P., Fjell, A.M., Ghisletta, P., Gorbach, T., Lindenberger, U.,
1084 Plachti, A., Walhovd, K.B., Nyberg, L., 2023. No moderating influence of education
1085 on the association between changes in hippocampus volume and memory performance
1086 in aging. Aging Brain 4, 100082. https://doi.org/10.1016/j.nbas.2023.100082
1087 Matsushima, J., Kawashima, T., Nabeta, H., Imamura, Y., Watanabe, I., Mizoguchi, Y.,
1088 Kojima, N., Yamada, S., Monji, A., 2015. Association of inflammatory biomarkers
1089 with depressive symptoms and cognitive decline in a community-dwelling healthy
1090 older sample: A 3-year follow-up study. J. Affect. Disord. 173, 9–14.
1091 https://doi.org/10.1016/j.jad.2014.10.030
1092 Monti, S., Tamayo, P., Mesirov, J., Golub, T., 2003. Consensus Clustering: A Resampling-
1093 Based Method for Class Discovery and Visualization of Gene Expression Microarray
1094 Data. Mach. Learn. 52, 91–118. https://doi.org/10.1023/A:1023949509487
1095 Morris, J.C., Heyman, A., Mohs, R.C., Hughes, J.P., van Belle, G., Fillenbaum, G., Mellits,
1096 E.D., Clark, C., 1989. The Consortium to Establish a Registry for Alzheimer's Disease
1097 (CERAD). Part I. Clinical and neuropsychological assessment of Alzheimer's disease.
1098 Neurology 39, 1159–1165. https://doi.org/10.1212/wnl.39.9.1159
1099 Mueller, S.G., Weiner, M.W., Thal, L.J., Petersen, R.C., Jack, C., Jagust, W., Trojanowski,
1100 J.Q., Toga, A.W., Beckett, L., 2005. The Alzheimer's disease neuroimaging initiative.
1101 Neuroimaging Clin. N. Am. 15, 869–877, xi–xii.
1102 https://doi.org/10.1016/j.nic.2005.09.008
1103 Nasreddine, Z.S., Phillips, N.A., Bédirian, V., Charbonneau, S., Whitehead, V., Collin, I.,
1104 Cummings, J.L., Chertkow, H., 2005. The Montreal Cognitive Assessment, MoCA: A

1105 Brief Screening Tool For Mild Cognitive Impairment. J. Am. Geriatr. Soc. 53, 695–
1106 699. https://doi.org/10.1111/j.1532-5415.2005.53221.x
1107 Ng, A., Jordan, M., Weiss, Y., 2001. On Spectral Clustering: Analysis and an algorithm, in:
1108 Advances in Neural Information Processing Systems. MIT Press.
1109 Nyberg, L., Andersson, M., Lundquist, A., 2023. Longitudinal change-change associations of
1110 cognition with cortical thickness and surface area. Aging Brain 3, 100070.
1111 https://doi.org/10.1016/j.nbas.2023.100070
1112 Nyberg, L., Lövdén, M., Riklund, K., Lindenberger, U., Bäckman, L., 2012. Memory aging
1113 and brain maintenance. Trends Cogn. Sci. 16, 292–305.
1114 https://doi.org/10.1016/j.tics.2012.04.005
1115 Nyberg, L., Magnussen, F., Lundquist, A., Baaré, W., Bartrés-Faz, D., Bertram, L., Boraxbekk,
1116 C.J., Brandmaier, A.M., Drevon, C.A., Ebmeier, K., Ghisletta, P., Henson, R.N.,
1117 Junqué, C., Kievit, R., Kleemeyer, M., Knights, E., Kühn, S., Lindenberger, U.,
1118 Penninx, B.W.J.H., Pudas, S., Sørensen, Ø., Vaqué-Alcázar, L., Walhovd, K.B., Fjell,
1119 A.M., 2021. Educational attainment does not influence brain aging. Proc. Natl. Acad.
1120 Sci. 118, e2101644118. https://doi.org/10.1073/pnas.2101644118
1121 Panizzon, M.S., Fennema-Notestine, C., Eyler, L.T., Jernigan, T.L., Prom-Wormley, E., Neale,
1122 M., Jacobson, K., Lyons, M.J., Grant, M.D., Franz, C.E., Xian, H., Tsuang, M., Fischl,
1123 B., Seidman, L., Dale, A., Kremen, W.S., 2009. Distinct genetic influences on cortical
1124 surface area and cortical thickness. Cereb. Cortex N. Y. N 1991 19, 2728–2735.
1125 https://doi.org/10.1093/cercor/bhp026
1126 Parent, C., Rousseau, L.-S., Predovan, D., Duchesne, S., Hudon, C., 2023. Longitudinal
1127 association between ß-amyloid accumulation and cognitive decline in cognitively
1128 healthy older adults: A systematic review. Aging Brain 3, 100074.
1129 https://doi.org/10.1016/j.nbas.2023.100074

1130 Persson, J., Pudas, S., Lind, J., Kauppi, K., Nilsson, L.-G., Nyberg, L., 2012. Longitudinal
1131 structure-function correlates in elderly reveal MTL dysfunction with cognitive decline.
1132 Cereb. Cortex N. Y. N 1991 22, 2297–2304. https://doi.org/10.1093/cercor/bhr306
1133 Pettigrew, C., Soldan, A., Sloane, K., Cai, Q., Wang, J., Wang, M.-C., Moghekar, A., Miller,
1134 M.I., Albert, M., 2017. Progressive medial temporal lobe atrophy during preclinical
1135 Alzheimer's disease. NeuroImage Clin. 16, 439–446.
1136 https://doi.org/10.1016/j.nicl.2017.08.022
1137 Pettigrew, C., Soldan, A., Zhu, Y., Wang, M.-C., Moghekar, A., Brown, T., Miller, M., Albert,
1138 M., 2016. Cortical thickness in relation to clinical symptom onset in preclinical AD.
1139 NeuroImage Clin. 12, 116–122. https://doi.org/10.1016/j.nicl.2016.06.010
1140 R Core Team, 2022. R: A Language and Environment for Statistical Computing. R core team.
1141 Rakic, P., 1988. Specification of cerebral cortical areas. Science 241, 170–176.
1142 https://doi.org/10.1126/science.3291116
1143 Randolph, C., Tierney, M.C., Mohr, E., Chase, T.N., 1998. The Repeatable Battery for the
1144 Assessment of Neuropsychological Status (RBANS): Preliminary Clinical Validity. J.
1145 Clin. Exp. Neuropsychol. 20, 310–319. https://doi.org/10.1076/jcen.20.3.310.823
1146 Raz, N., Lindenberger, U., 2011. Only Time will Tell: Cross-sectional Studies Offer no
1147 Solution to the Age-Brain-Cognition Triangle—Comment on. Psychol. Bull. 137, 790–
1148 795. https://doi.org/10.1037/a0024503
1149 Reuter, M., Rosas, H.D., Fischl, B., 2010. Highly accurate inverse consistent registration: A
1150 robust approach. NeuroImage 53, 1181–1196.
1151 https://doi.org/10.1016/j.neuroimage.2010.07.020
1152 Reuter, M., Schmansky, N.J., Rosas, H.D., Fischl, B., 2012. Within-subject template estimation
1153 for unbiased longitudinal image analysis. NeuroImage 61, 1402–1418.
1154 https://doi.org/10.1016/j.neuroimage.2012.02.084

1155 Routier, A., Burgos, N., Díaz, M., Bacci, M., Bottani, S., El-Rifai, O., Fontanella, S., Gori, P.,
1156 Guillon, J., Guyot, A., Hassanaly, R., Jacquemont, T., Lu, P., Marcoux, A., Moreau, T.,
1157 Samper-González, J., Teichmann, M., Thibeau-Sutre, E., Vaillant, G., Wen, J., Wild,
1158 A., Habert, M.-O., Durrleman, S., Colliot, O., 2021. Clinica: An Open-Source Software
1159 Platform for Reproducible Clinical Neuroscience Studies. Front. Neuroinformatics 15,
1160 689675. https://doi.org/10.3389/fninf.2021.689675
1161 Salthouse, T.A., 2014. Selectivity of Attrition in Longitudinal Studies of Cognitive
1162 Functioning. J. Gerontol. B. Psychol. Sci. Soc. Sci. 69, 567–574.
1163 https://doi.org/10.1093/geronb/gbt046
1164 Samper-González, J., Burgos, N., Bottani, S., Fontanella, S., Lu, P., Marcoux, A., Routier, A.,
1165 Guillon, J., Bacci, M., Wen, J., Bertrand, A., Bertin, H., Habert, M.-O., Durrleman, S.,
1166 Evgeniou, T., Colliot, O., 2018. Reproducible evaluation of classification methods in
1167 Alzheimer's disease: Framework and application to MRI and PET data. NeuroImage
1168 183, 504–521. https://doi.org/10.1016/j.neuroimage.2018.08.042
1169 Sele, S., Liem, F., Mérillat, S., Jäncke, L., 2021. Age-related decline in the brain: a longitudinal
1170 study on inter-individual variability of cortical thickness, area, volume, and cognition.
1171 NeuroImage 240, 118370. https://doi.org/10.1016/j.neuroimage.2021.118370
1172 Sele, S., Liem, F., Mérillat, S., Jäncke, L., 2020. Decline Variability of Cortical and Subcortical
1173 Regions in Aging: A Longitudinal Study. Front. Hum. Neurosci. 14.
1174 Sim, J., Wright, C.C., 2005. The Kappa Statistic in Reliability Studies: Use, Interpretation, and
1175 Sample Size Requirements. Phys. Ther. 85, 257–268.
1176 https://doi.org/10.1093/ptj/85.3.257
1177 Stern, Y., 2012. Cognitive reserve in ageing and Alzheimer's disease. Lancet Neurol. 11, 1006–
1178 1012. https://doi.org/10.1016/S1474-4422(12)70191-6

1179 Stern, Y., Barnes, C.A., Grady, C., Jones, R.N., Raz, N., 2019. Brain reserve, cognitive reserve,
1180 compensation, and maintenance: operationalization, validity, and mechanisms of
1181 cognitive resilience. Neurobiol. Aging 83, 124–129.
1182 https://doi.org/10.1016/j.neurobiolaging.2019.03.022
1183 Stomrud, E., Hansson, O., Blennow, K., Minthon, L., Londos, E., 2007. Cerebrospinal Fluid
1184 Biomarkers Predict Decline in Subjective Cognitive Function over 3 Years in Healthy
1185 Elderly. Dement. Geriatr. Cogn. Disord. 24, 118–124.
1186 https://doi.org/10.1159/000105017
1187 Storsve, A.B., Fjell, A.M., Tamnes, C.K., Westlye, L.T., Overbye, K., Aasland, H.W.,
1188 Walhovd, K.B., 2014. Differential Longitudinal Changes in Cortical Thickness,
1189 Surface Area and Volume across the Adult Life Span: Regions of Accelerating and
1190 Decelerating Change. J. Neurosci. 34, 8488–8498.
1191 https://doi.org/10.1523/JNEUROSCI.0391-14.2014
1192 Stricker, N.H., Dodge, H.H., Dowling, N.M., Han, S.D., Erosheva, E.A., Jagust, W.J., for the
1193 Alzheimer's Disease Neuroimaging Initiative, 2012. CSF biomarker associations with
1194 change in hippocampal volume and precuneus thickness: implications for the
1195 Alzheimer's pathological cascade. Brain Imaging Behav. 6, 599–609.
1196 https://doi.org/10.1007/s11682-012-9171-6
1197 Svenningsson, A.L., Stomrud, E., Insel, P.S., Mattsson, N., Palmqvist, S., Hansson, O., 2019.
1198 β-amyloid pathology and hippocampal atrophy are independently associated with
1199 memory function in cognitively healthy elderly. Sci. Rep. 9, 11180.
1200 https://doi.org/10.1038/s41598-019-47638-y
1201 Takao, H., Hayashi, N., Ohtomo, K., 2012. A longitudinal study of brain volume changes in
1202 normal aging. Eur. J. Radiol. 81, 2801–2804.
1203 https://doi.org/10.1016/j.ejrad.2011.10.011

1204 Thambisetty, M., Wan, J., Carass, A., An, Y., Prince, J.L., Resnick, S.M., 2010. Longitudinal
1205 changes in cortical thickness associated with normal aging. NeuroImage 52, 1215–
1206 1223. https://doi.org/10.1016/j.neuroimage.2010.04.258
1207 Thompson, P.M., Hayashi, K.M., De Zubicaray, G.I., Janke, A.L., Rose, S.E., Semple, J.,
1208 Hong, M.S., Herman, D.H., Gravano, D., Doddrell, D.M., Toga, A.W., 2004. Mapping
1209 hippocampal and ventricular change in Alzheimer disease. NeuroImage 22, 1754–1766.
1210 https://doi.org/10.1016/j.neuroimage.2004.03.040
1211 Tibshirani, R., 1996. Regression Shrinkage and Selection via the Lasso. J. R. Stat. Soc. Ser. B
1212 Methodol. 58, 267–288.
1213 Tosun, D., Schuff, N., Shaw, L.M., Trojanowski, J.Q., Weiner, M.W., 2011. Relationship
1214 Between CSF Biomarkers of Alzheimer's Disease and Rates of Regional Cortical
1215 Thinning in ADNI Data. J. Alzheimers Dis. JAD 26, 77–90.
1216 https://doi.org/10.3233/JAD-2011-0006
1217 Tremblay-Mercier, J., Madjar, C., Das, S., Pichet Binette, A., Dyke, S.O.M., Étienne, P.,
1218 Lafaille-Magnan, M.-E., Remz, J., Bellec, P., Louis Collins, D., Natasha Rajah, M.,
1219 Bohbot, V., Leoutsakos, J.-M., Iturria-Medina, Y., Kat, J., Hoge, R.D., Gauthier, S.,
1220 Tardif, C.L., Mallar Chakravarty, M., Poline, J.-B., Rosa-Neto, P., Evans, A.C.,
1221 Villeneuve, S., Poirier, J., Breitner, J.C.S., PREVENT-AD Research Group, 2021.
1222 Open science datasets from PREVENT-AD, a longitudinal cohort of pre-symptomatic
1223 Alzheimer's disease. NeuroImage Clin. 31, 102733.
1224 https://doi.org/10.1016/j.nicl.2021.102733
1225 Vidal-Piñeiro, D., Sørensen, Ø., Blennow, K., Capogna, E., Halaas, N.B., Idland, A.-V.,
1226 Mowinckel, A.M., Pereira, J.B., Watne, L.O., Zetterberg, H., Walhovd, K.B., Fjell,
1227 A.M., 2022. Relationship between cerebrospinal fluid neurodegeneration biomarkers

and temporal brain atrophy in cognitively healthy older adults. Neurobiol. Aging 116, 80–91. https://doi.org/10.1016/j.neurobiolaging.2022.04.010

Walhovd, K.B., Krogsrud, S.K., Amlien, I.K., Bartsch, H., Bjørnerud, A., Due-Tønnessen, P., Grydeland, H., Hagler, D.J., Håberg, A.K., Kremen, W.S., Ferschmann, L., Nyberg, L., Panizzon, M.S., Rohani, D.A., Skranes, J., Storsve, A.B., Sølsnes, A.E., Tamnes, C.K., Thompson, W.K., Reuter, C., Dale, A.M., Fjell, A.M., 2016. Neurodevelopmental origins of lifespan changes in brain and cognition. Proc. Natl. Acad. Sci. 113, 9357–9362. https://doi.org/10.1073/pnas.1524259113

Walhovd, K.B., Lövden, M., Fjell, A.M., 2023. Timing of lifespan influences on brain and cognition. Trends Cogn. Sci. S1364-6613(23)00169–9. https://doi.org/10.1016/j.tics.2023.07.001

Walhovd, K.B., Nyberg, L., Lindenberger, U., Amlien, I.K., Sørensen, Ø., Wang, Y., Mowinckel, A.M., Kievit, R.A., Ebmeier, K.P., Bartrés-Faz, D., Kühn, S., Boraxbekk, C.-J., Ghisletta, P., Madsen, K.S., Baaré, W.F.C., Zsoldos, E., Magnussen, F., Vidal-Piñeiro, D., Penninx, B., Fjell, A.M., 2022. Brain aging differs with cognitive ability regardless of education. Sci. Rep. 12, 13886. https://doi.org/10.1038/s41598-022-17727-6

Wang, L., Benzinger, T.L., Hassenstab, J., Blazey, T., Owen, C., Liu, J., Fagan, A.M., Morris, J.C., Ances, B.M., 2015. Spatially distinct atrophy is linked to β-amyloid and tau in preclinical Alzheimer disease. Neurology 84, 1254–1260. https://doi.org/10.1212/WNL.0000000000001401

Wechsler, D., 1987. Wechsler Memory Scale-Revised. Psychol. Corp.

Westfall, F.B., Torsten Hothorn, Peter, 2010. Multiple Comparisons Using R. Chapman and Hall/CRC, New York. https://doi.org/10.1201/9781420010909

1252 Wisse, L.E., Xie, L., Das, S.R., de Flores, R., Hansson, O., Habes, M., Doshi, J., Davatzikos,
1253 C., Yushkevich, P.A., Wolk, D.A., 2022. Tau pathology mediates age effects on medial
1254 temporal lobe structure. Neurobiol. Aging 109, 135–144.
1255 https://doi.org/10.1016/j.neurobiolaging.2021.09.017
1256 Wood, S.N., 2017. Generalized Additive Models: An Introduction with R, Second Edition, 2nd
1257 ed. Chapman and Hall/CRC, Boca Raton. https://doi.org/10.1201/9781315370279
1258 Yang, Y., Zou, H., 2015. A fast unified algorithm for solving group-lasso penalize learning
1259 problems. Stat. Comput. 25, 1129–1141. https://doi.org/10.1007/s11222-014-9498-5
1260 Zuo, X.-N., Xu, T., Milham, M.P., 2019. Harnessing reliability for neuroscience research. Nat.
1261 Hum. Behav. 3, 768–771. https://doi.org/10.1038/s41562-019-0655-x
1262